Article:
Sakurai, Masatoshi, Ishitsuka, Kantaro, Ito, Ryoji et al. (17 more authors) (2023) Chemically defined cytokine-free expansion of human haematopoietic stem cells. Nature. pp. 127-133. ISSN 0028-0836

https://doi.org/10.1038/s41586-023-05739-9

Chemically-defined cytokine-free human hematopoietic stem cell expansion

Authors:

Masatoshi Sakurai[1,2*], Kantaro Ishitsuka[3*], Ryoji Ito[4], Adam C Wilkinson[1,5,6], Takaharu Kimura[3], Eiji Mizutani[3,7], Hidekazu Nishikii[8], Kazuhiro Sudo[9], Hans Jiro Becker[1,3], Hiroshi Takemoto[10], Tsubasa Sano[11], Keisuke Kataoka[2,12], Satoshi Takahashi[13], Yukio Nakamura[9], David G Kent[14,15], Atsushi Iwama[16], Shigeru Chiba[8], Shinichiro Okamoto[2], Hiromitsu Nakauchi[6,7,17], and Satoshi Yamazaki[1,3,17]

Affiliations:

[1]Division of Stem Cell Biology, Center for Stem Cell Biology and Regenerative Medicine, The Institute of Medical Science, The University of Tokyo, Japan

[2]Division of Hematology, Department of Medicine, Keio University School of Medicine, Tokyo, Japan

[3]Laboratory of Stem Cell Therapy, Faculty of Medicine, University of Tsukuba, Ibaraki, Japan

[4]Human Disease Model Laboratory, Central Institute for Experimental Animals, Kawasaki, Kanagawa, Japan

[5]MRC Weatherall Institute of Molecular Medicine, University of Oxford, Oxford, UK

[6]Institute for Stem Cell Biology and Regenerative Medicine, Department of Genetics, Stanford University School of Medicine, Lorry I. Lokey Stem Cell Research Building, 265 Campus Drive, Stanford, CA, USA

[7]Division of Stem Cell Therapy, Distinguished Professor Unit, The Institute of Medical Science, The University of Tokyo, Tokyo, Japan

[8]Department of Hematology, Faculty of Medicine, University of Tsukuba, Ibaraki, Japan.

[9]Cell Engineering Division, RIKEN BioResource Research Center, Tsukuba, Japan.

[10]Department of Neuroscience, Drug Discovery & Disease Research Laboratory, Shionogi; Business-Academia Collaborative Laboratory (Shionogi), Graduate School of Pharmaceutical Sciences, The University of Tokyo, Japan

[11]Pharma Solutions, Nutrition & Health, BASF Japan Ltd., Tokyo, Japan

[12]Division of Molecular Oncology, National Cancer Center Research Institute, Tokyo, Japan

[13]Division of Clinical Precision Research Platform, The Institute of Medical Science, The University of Tokyo, Tokyo, Japan
[14]Department of Biology, York Biomedical Research Institute, University of York, York, UK
[15]Wellcome MRC Cambridge Stem Cell Institute, University of Cambridge, Cambridge, UK
[16]Division of Stem Cell and Molecular Medicine, Center for Stem Cell Biology and Regenerative Medicine, The Institute of Medical Science, The University of Tokyo, Japan
[17]Corresponding authors. Email: y-sato4@md.tsukuba.ac.jp (S.Y.); nakauchi@stanford.edu (H.N.)
*These authors contributed equally.

Keywords: Human hematopoietic stem cell; ex vivo expansion; chemically defined; PI3K activator; polyvinyl caprolactam-polyvinyl acetate-polyethylene glycol graft copolymer.

Abstract:

Hematopoietic stem cells (HSCs) are a rare cell type that reconstitute the entire blood and immune systems following transplantation, a curative cell therapy for a variety of hematological diseases[1,2]. However, the low number of HSCs makes both biological analyses and clinical application difficult, and the limited ability to expand human HSCs ex vivo remains a substantial barrier to the wider and safer therapeutic use of HSCT[3]. While various reagents have been tested in attempts to stimulate human HSC expansion, cytokines have long been thought to be essential for supporting HSCs ex vivo[4]. Here we report the establishment of a novel culture system that supports the long-term ex vivo expansion of human HSCs, achieved through the complete replacement of exogenous cytokines and albumin with chemical agonists and a caprolactam-based polymer. A phosphoinositide 3-kinase activator, in combination with a thrombopoietin-receptor agonist and the pyrimidoindole derivative UM171 were sufficient to stimulate expansion of umbilical cord blood HSCs capable of serial engraftment in xenotransplantation assays. Ex vivo HSC expansion was further supported by split-clone transplantation assays and single cell RNA-sequencing analysis. We envision that this chemically-defined expansion culture system will help to advance clinical HSC therapies.

Main text:

Self-renewing multipotent hematopoietic stem cells (HSCs) are a rare bone marrow (BM) cell population that support life-long hematopoiesis[5-8] and hematopoietic system reconstitution following HSC transplantation (HSCT) [1]. HSCs can also be collected from umbilical cord blood (CB), which represents a highly-accessible source for transplantation but often contain too few HSCs for successful engraftment and durable hematopoietic reconstitution. Ex vivo expansion of human HSCs, particularly CB-derived HSCs, is therefore a major goal in hematology and one that remains a substantial barrier to the wider and safer therapeutic use of HSCs[3].

Various recombinant cytokines are commonly added to human HSC cultures in attempts to promote HSC expansion, usually in combination with serum albumin[4]. These cultures generally support short-term maintenance of HSCs but fail to expand functional HSCs. However, two-week ex vivo expansion of human HSCs has been achieved by the addition of small molecules, StemRegenin 1 (SR-1) [9] and UM171[10]. Clinical trials using these approaches to expand CB HSCs prior to transplantation have reported encouraging results[2,11]. Other recent approaches have included use of 3-dimensional zwitterionic hydrogels[12], addition of novel growth factors[13], or combinations of small molecule inhibitors[14]. These methods have highlighted the importance of collaboration between chemical biology and stem cell biology to overcome this major barrier in hematology.

A chemically-defined cytokine-free media

Working towards the goal of expanding HSCs ex vivo, we recently established a long-term ex vivo expansion system for functional mouse HSCs by optimizing the concentrations of recombinant stem cell factor (SCF) and thrombopoietin (THPO), and replacing serum albumin for the synthetic polymer polyvinyl alcohol (PVA) [15,16]. Use of PVA avoided the batch-to-batch variability associated with serum albumin[17] and culture contamination with albumin-associated impurities that promote HSC differentiation. While mouse HSCs expanded rapidly in these conditions, human HSC expansion was more limited. When we compared the proliferation of mouse BM $Kit^{+}Sca\text{-}1^{+}Linage^{-}$ (KSL) HSPCs with human CB $CD34^{+}CD38^{-}$ HSPCs in PVA-based media supplemented with SCF and THPO[15], mouse HSPCs proliferated ~18-fold in 7 days while human

HSPCs only proliferated ~3-4-fold during the same time (**Figure 1a**). To examine the difference between mouse and human HSPCs during these cultures, we analyzed the phosphorylation status of major signaling pathways (PI3K, JAK/STAT, MAPK) linked to SCF and THPO signaling[8,18,19]. Significant decreases in PI3K and AKT were observed in human cells (**Figure 1b**, **Extended Data Figure 1a, b**). The PI3K phosphorylation signal was also significantly decreased in human $CD34^+CD38^-CD90^+CD45RA^-CD49f^+$ phenotypic HSCs (**Extended Data Figure 1c**).

Based on these results, we hypothesized that we could improve human HSPC expansion by activating PI3K-AKT signaling. We therefore evaluated chemical agonists 740Y-P (a PI3K activator) and SC79 (an AKT activator) in human HSPC cultures. While SC79 did not improve expansion efficacy, 740Y-P significantly increased the number of $CD34^+$ cells (**Figure 1c**) and $CD34^+CD45RA^-$ cells in 7-day cultures (**Extended Data Figure 1d**). Furthermore, addition of 740Y-P significantly increased PI3K phosphorylation in $CD34^+CD38^-CD90^+CD45RA^-CD49f^+$ cells (**Extended Data Figure 1e**). These results suggested that chemical activation of the PI3K pathway was sufficient to improve human HSPC proliferation.

Previous studies have shown that SCF stimulates HSC cell cycle entry via the PI3K/AKT/FOXO pathway[20-23]. We therefore hypothesized that we could replace SCF with 740Y-P in human $CD34^+$ HSPCs cultures. No significant differences were observed in the 7-day cell proliferation in THPO and 740Y-P with or without SCF (**Figure 1d**), suggesting that SCF can be replaced with a PI3K activator. Cell cycle analysis confirmed that the frequency of S/G2/M cells was comparable (**Extended Data Figure 1f**) while colony forming unit (CFU) assays showed similar increases in multipotent granulocyte-erythrocyte-monocyte-megakaryocyte (GEmM) CFUs in the presence or absence of SCF (**Extended Data Figure 1g**). These results suggested that SCF was replaceable with 740Y-P in ex vivo human HSPC cultures.

We previously reported that recombinant proteins could destabilize HSC cultures[15]. Recently, we found that chemical THPO receptor agonists (THPO-RAs) could be used to induce human HSC expansion[24]. We therefore examined whether we could replace recombinant THPO with THPO-RAs in PVA-based media containing 740Y-P. Initial screening for optimal THPO-RAs was performed using a THPO-dependent MPL-

expressing cell line reported to proliferate in THPO-supplemented PVA conditions[25]. Of the three THPO-RAs tested, only butyzamide supported cell proliferation (**Extended Data Figure 1h**). We validated that butyzamide stimulated human $CD34^+$ cell proliferation in PVA-based media containing 740Y-P (**Extended Data Figure 1i**). Surprisingly, when compared to the THPO and 740Y-P cultures, the butyzamide and 740Y-P cultures displayed significantly improved 7-day proliferation (total, $CD34^+$ and $CD34^+CD41^-CD90^+CD45RA^-$ cell numbers) and GEmM CFU numbers (**Figure 1e, Extended Data Figure 1j, k**). However, there was no additive effect of THPO and butyzamide (**Extended Data Figure 1j**). In summary, these results confirmed that human $CD34^+$ HSPCs could be grown without exogenous cytokines by replacing SCF and THPO with 740Y-P and butyzamide, respectively.

We next titrated 740Y-P and butyzamide concentrations for $CD34^+$ cell expansion and identified the combination of 1 μM 740Y-P and 0.1 μM butyzamide as optimal for cell expansion, in terms of both total and $CD34^+$ cell expansion (**Figure 1f**). We defined this combination of 740Y-P (1 μM) and butyzamide (0.1 μM) as two activators (2a) media. Using this media composition, we next examined long-term stability of $CD34^+$ cell cultures. Although total cell numbers increased during 14-day cultures, the number of phenotypic $CD34^+$ cells decreased between day 7 and 14, and the cultures became dominated by $CD41^+$ cells (**Figure 1g**, **Extended Data Figure 1l**). Consistent with accumulation of these $CD41^+$ megakaryocyte-lineage cells (**Extended Data Figure 1m**), significant increases in megakaryocyte (MgK) CFUs were observed in the day 14 cultures (**Extended Data Figure 1n**). Additionally, while $1x10^4$ cells from 7-day 2a cultures engrafted robustly in immunodeficient NOD/Shi-scid IL-2Rγ^{null} (NOG) mice[26], chimerism was not detected from 14-day 2a cultures (**Extended Data Figure 1o, p**). Together, these results suggested that although 2a cytokine-free media supported human HSCs short-term, it was not sufficient to stabilize longer-term expansion.

Long-term ex vivo HSC cultures

Based on our 2a culture results, we searched for potential MgK inhibitors to stabilize long-term ex vivo HSC expansion. We evaluated two reported HSPC expansion compounds, SR-1[9] and UM171[10]. Addition of UM171 increased the total, $CD34^+$ and

$CD34^+EPCR^+$ cell numbers after 7-days (**Figure 2a, Extended Data Figure 2a**). In 14-day UM171 supplemented cultures, total, $CD34^+$, $CD34^+EPCR^+$ and $CD34^+EPCR^+CD90^+CD45RA^-ITGA3^+$ cells were significantly increased while $CD41^+$ cell numbers were reduced (**Figure 2b, Extended Data Figure 2b**). Furthermore, the expansion of $CD34^+EPCR^+CD90^+CD45RA^-ITGA3^+$ cells was significantly higher with UM171 at 70 nM as compared to than 35 nM (**Extended Data Figure 2c**). Meanwhile, the addition of SR-1 induced apoptosis (**Extended Data Figure 2d**). This three activator (3a) media cocktail of UM171 (70 nM), 740Y-P (1 μM) and butyzamide (0.1 μM) continued to stimulate proliferation over a 30-day culture by ~14-fold (**Figure 2c**). These results suggested that HSPCs may be stably expanding in the 3a media.

To evaluate the in vivo engraftment and differentiation potential of the cultured HSPCs, we performed xenotransplantation assay. We transplanted $1x10^4$ $CD34^+$ cells before culture (fresh) and after 10-day or 30-day cultures. Significantly higher human $CD45^+$ PB chimerism was observed in the 10-day and 30-day culture groups, with chimerism increasing over time (**Figure 2d, Extended Data Figure 2e**). BM analysis at 16- and 24-weeks also identified significantly higher human cell chimerism in the cultured HSPC groups (**Figure 2e, Extended Data Figure 2f**); human $CD45^+$ chimerism from the fresh group was ~3%, while 10-day and 30-day culture groups displayed ~70% and ~85% chimerism, respectively (**Figure 2e**). The frequency of human $CD34^+$ cells in the BM and spleen at 16- and 24-weeks was also significantly higher in the 10- or 30-day culture group (**Figure 2f, Extended Data Figure 2f-g**, where multilineage output was also observed (**Extended Data Table 1a**). These results confirmed that our cytokine-free 3a media could maintain and expand functional human HSCs for at least one-month ex vivo.

Caprolactam polymers improve HSC growth

Having established an albumin- and cytokine-free human HSC culture system, we next aimed to improve the rate of HSPC expansion ex vivo. The PVA-based 3a media only supported ~10-fold expansion of $CD34^+$ cells over 30 days, suggesting that further improvement was required. We hypothesized that other synthetic polymers might be more suitable for human HSC expansion. We therefore screened 10 polymers and identified

Soluplus®, a polyvinyl caprolactam-polyvinyl acetate-polyethylene glycol graft copolymer (PCL-PVAc-PEG) [27,28], as supportive of significantly higher cell expansion (**Figure 3a**). In PCL-PVAc-PEG-based cultures, the combination of 740Y-P, butyzamide, and UM171 was as effective as in the PVA-based cultures (**Extended Data Figure 3a-f**). However, the toxicity of SR-1 was significantly reduced compared to the PVA condition (**Extended Data Figure 3g**). PCL-PVAc-PEG-based 3a media also supported faster cell proliferation longer-term, with a ~75-fold expansion of total cells and ~55-fold expansion of $CD34^+$ cell observed after a 30-day culture (**Figure 3b**). The addition of a PI3K inhibitor led to cell death, suggesting that cell expansion was dependent on the PI3K/AKT signaling (**Extended Data Figure 3h**). Furthermore, PVA- and PCL-PVAc-PEG-based 3a media also supported ex vivo expansion of adult-PBSC $CD34^+$ cells, with a ~8-10-fold expansion of total cells observed after a 10-day culture (**Extended Data Figure 3i**).

To compare in vivo engraftment and differentiation potential of the PCL-PVAc-PEG and PVA cultured HSPCs, we performed xenotransplantation assays. We transplanted $1x10^4$ cells per recipient from day-30 3a media cultures containing PVA and/or PCL-PVAc-PEG. Interestingly, similar robust human cell chimerism was observed from all conditions, including in the PB, BM, and spleen (**Figure 3c-e, Extended Data Figure 3j-l, Extended Data Table 1b, Supplementary Table 1**). Robust human $CD45^+$ chimerism was also observed in secondary xenotransplantation recipients (**Figure 3f-g, Supplementary Table 2**). However, lymphoid bias was observed due to the characteristics of the NOG mice[26,29]. We re-performed the xenotransplantation assays using human IL-3/GM-CSF-transgenic NOG (NOG IL-3/GM-Tg) mice[30]. In this context, we observed robust engraftment from long-term PCL-PVAc-PEG-based 3a cultures, with $CD33^+$ myeloid cells at 27% of human $CD45^+$ cells at 16-weeks post-transplantation (**Figure 3h, i**).

We next compared 10-day $CD34^+$ cell expansion in PCL-PVAc-PEG-based 3a media against published serum albumin-based media (StemSpan SFEM supplemented with cytokines and SR1 or UM171). While the total number of cells generated in the 10-day cultures was ~50% in 3a media (**Extended Data Figure 4a**), the frequency and absolute number of $CD34^+EPCR^+CD90^+CD45RA^-ITGA3^+$ cells was strikingly increased

(**Extended Data Figure 4b, c**). PCL-PVAc-PEG-based 3a media was also superior to PCL-PVAc-PEG-based cytokine cocktail media (**Extended Data Figure 4b, c**). Consistent with higher metabolic activity and active cell division, all culture conditions caused an increase in ROS and yH2AX compared to fresh $CD34^+$ cells (**Extended Data Figure 4d**); however, these did not accumulate further in longer-term 30-day 3a cultures (**Extended Data Figure 4e**). Corresponding with the increased frequency of HSPCs, the 3a cultured cells also demonstrated significantly higher human $CD45^+$ PB and BM chimerism following transplantation of $1x10^4$ 10-day cultured cells into recipient NOG mice (**Extended Data Figure 4f, g**). Human $CD45^+$ chimerism was detected in the PB and BM of 1/3 secondary transplantation recipients at 24-weeks post-transplantation (**Extended Data Figure 4h, i**). It is worth noting that our xenotransplantation assay protocol differs to those used in the development of SR-1[11], which may account for the differences in engraftment. Nonetheless, these results confirmed that 3a media support robust expansion of functionally engraftable human HSCs ex vivo.

Long-term selective HSC expansion

The robust in vivo engraftment potential of these human HSC cultures suggested that a high frequency of HSCs was maintained within the 3a cultures. To further investigate the composition of these long-term HSPC cultures, we performed flow cytometric analysis of HSC-associated surface markers. This revealed a striking enrichment of phenotypic HSCs after PCL-PVAc-PEG culture, with the $CD34^+EPCR^+CD90^+CD45RA^-ITGA3^+$ cell fraction significantly enriched after 7-day cultures (**Extended Data Figure 4b-c, Extended Data Figure 5a**).

We also sought to characterize the PCL-PVAc-PEG based 3a cultures at the molecular level. We performed whole exome sequencing on fresh and 10-day cultured CB $CD34^+$ cells and detected seven mutations that could a cause amino acid change and four mutations that were located on a splice site in cultured cells (**Extended Data Table 2**). To the best of our knowledge, these mutations are not involved in hematological malignancies nor clonal hematopoiesis. These results support the safety of our culture system, and suggest further clinical development is warranted.

We next performed bulk RNA sequencing on CD34^{high}EPCR^{+} and CD34^{high}EPCR^{-} cells from 10-day cultures. EPCR expression is known to mark LT-HSCs in UM171-supplemented media[31]. Consistent with previous studies[32], expression of LT-HSC markers *HLF* and *AVP* were enriched in the CD34^{high}EPCR^{+} fraction (**Extended Data Figure 5b**). Additional HSC genes, *PRDM16*[33] and *FGD5*[34], were also upregulated in the CD34^{high}EPCR^{+} fraction (**Figure 4a**) and Gene Set Enrichment Analysis (GSEA) confirmed that HSC gene sets were upregulated in the CD34^{high}EPCR^{+} fraction (**Figure 4b**). GSEA also revealed that lysosomal membrane related genes were enriched in CD34^{high}EPCR^{+} cells (**Extended Data Figure 6b**), consistent with a report that lysosomal activity against various external signals has an important role in the self-renewal of human LT-HSCs[35]. On the other hand, oxidative phosphorylation (OXPHOS) and mitochondrial ribosomes genes were upregulated in CD34^{high}EPCR^{-} cells (**Figure 4c, Extended Data Figure 6b**), consistent with a report that high mitochondrial membrane potential (MMP) HSCs had less intracellular lysosomal contents than quiescent MMP-low LT-HSCs[36].

To further resolve the cellular heterogeneity within the HSC cultures, we used single-cell RNA sequencing to compare our 3a conditions with StemSpan SFEM supplemented with cytokines and SR1 or UM171[2,11]. After integration and analysis of these three samples using Seurat, we identified and manually annotated 12 major clusters (**Figure 4d, Extended Data Figure 6c**). This included a population of cells expressing HSC genes, *HLF* and *AVP*, while lacking expression lineage-specific genes (*MPO*, *ITGA2B*), which we termed HSPC-HLF (**Figure 4d, Extended Data Figure 6c-e**). Lower expression of *HLF* and *AVP* were also seen in two other populations (HSPC, HSPC-cycling), suggesting these to be intermediate stem/progenitor populations (**Extended Data Figure 6c**). Various downstream progenitor cell types, including erythroid, MgK, monocyte (Mon) and granulocyte (Gra) progenitors could also be identified (**Figure 4d, Extended Data Figure 6c**). Comparing the cellular composition of the 3a media and other two cytokine-based conditions (StemSpan SFEM with SR-1 or UM171), differences were apparent. In particular, high frequencies of the HSPC-HLF cluster and erythroid/MgK progenitors were observed in the 3a media, while the Mon and Gra progenitor clusters were generally depleted (**Figure 4e, Extended Data Figure 6f**). Similar results for the UM171 cultures were seen when we overlayed published single-

cell RNA-seq datasets onto our dataset (**Extended Data Figure 6g**). These results suggest that 3a culture conditions were more suitable for selective expansion of LT-HSCs. These differences in the cellular composition corresponded with the higher engraftment potential seen in the 3a media (**Extended Data Figure 4f, g**) and confirmed the highly selective nature of these cultures. In addition, 10-day cultured cells in 3a media had higher levels of *HLF* expression as compared to fresh CB $CD34^+$ cell samples[32] (**Extended Data Figure 6h**).

Finally, we examined whether 3a media could support the expansion of clonally-derived HSC cultures. Single CB-derived $CD34^+CD38^-CD90^+CD45RA^-CD49f^+$ cells were sorted into 96-well plates and cultured with PCL-PVAc-PEG-based 3a media. After 7 days, xenotransplantation assays were performed using NOD.Cg-$Prkdc^{scid}Il2rg^{tm1Sug}Kit^{em1(V831M)Jic}$/Jic (W41/W41) recipient mice (**Figure 4f**), which support higher human hematopoietic cell chimerism in xenotransplantation assays (**Extended Data Figure 8**). Although heterogeneous clonal expansion was observed, 20 out of 96 wells (21%) expanded more than 10-fold and 11 out of 96 wells (11%) expanded over 30-fold in 7 days (**Figure 4f, Supplementary Table 3**). The 10 wells with the highest expansion rate were transplanted into individual recipients. Five out of the ten recipients displayed robust PB, BM, and spleen chimerism with over 5% multilineage human $CD45^+$ chimerism in the BM and spleen after 24-weeks (**Figure 4h, i, Extended Data Table 1c Supplementary Table 4**). Furthermore, we performed split clone experiments by transplanting single HSC-derived cultures into three W41/W41 mice using HSC clones that displayed more than 10-fold expansion by day 7. For three out of six clones, all three recipients showed human cell engraftment (**Extended Data Figure 7a, b**), confirming that clonal amplification of HSCs is supported by the 3a media. Together, these results confirm that PCL-PVAc-PEG-based 3a media can support both bulk and clonal expansion of human HSCs ex vivo.

Discussion

Here, we report a recombinant cytokine-free albumin-free long-term expansion culture system for human HSCs. These conditions selectively expanded functional HSPCs for at least 30 days ex vivo and also supported clonal HSC expansion, which may

contribute to efforts to decipher the heterogeneity of the human HSC compartment in health and disease[37]. As highlighted by recent clinical trials[2,11], the ability to expand CB HSPCs ex vivo has important implications for solving the shortage of donor HSCs for allogeneic HSCT. In this regard, 3a media may hold advantages in being recombinant protein-free and chemically defined, which should improve batch-to-batch variability, reduce reagent costs and facilitate rapid clinical translation. However, further comparison of human HSC culture methods are warranted. In conclusion, this culture system provides a powerful platform for both basic scientists and clinicians interested in stem cell biology and HSC therapies.

References:

1 Copelan, E. A. Hematopoietic stem-cell transplantation. *N Engl J Med* **354**, 1813-1826, doi:10.1056/NEJMra052638 (2006).

2 Cohen, S. *et al.* Hematopoietic stem cell transplantation using single UM171-expanded cord blood: a single-arm, phase 1-2 safety and feasibility study. *Lancet Haematol* **7**, e134-e145, doi:10.1016/s2352-3026(19)30202-9 (2020).

3 Pineault, N. & Abu-Khader, A. Advances in umbilical cord blood stem cell expansion and clinical translation. *Exp Hematol* **43**, 498-513, doi:10.1016/j.exphem.2015.04.011 (2015).

4 Wilkinson, A. C. & Nakauchi, H. Stabilizing hematopoietic stem cells in vitro. *Current Opinion in Genetics & Development* **64**, 1 - 5, doi:https://doi.org/10.1016/j.gde.2020.05.035 (2020).

5 Gluckman, E. *et al.* Hematopoietic reconstitution in a patient with Fanconi's anemia by means of umbilical-cord blood from an HLA-identical sibling. *N Engl J Med* **321**, 1174-1178, doi:10.1056/nejm198910263211707 (1989).

6 Orkin, S. H. & Zon, L. I. Hematopoiesis: an evolving paradigm for stem cell biology. *Cell* **132**, 631-644, doi:10.1016/j.cell.2008.01.025 (2008).

7 Weissman, I. L. Stem cells: units of development, units of regeneration, and units in evolution. *Cell* **100**, 157-168, doi:10.1016/s0092-8674(00)81692-x (2000).

8 Wilkinson, A. C., Igarashi, K. J. & Nakauchi, H. Haematopoietic stem cell self-renewal in vivo and ex vivo. *Nat Rev Genet*, doi:10.1038/s41576-020-0241-0 (2020).

9 Boitano, A. E. *et al.* Aryl hydrocarbon receptor antagonists promote the expansion of human hematopoietic stem cells. *Science* **329**, 1345-1348, doi:10.1126/science.1191536 (2010).

10 Fares, I. *et al.* Cord blood expansion. Pyrimidoindole derivatives are agonists of human hematopoietic stem cell self-renewal. *Science* **345**, 1509-1512, doi:10.1126/science.1256337

(2014).

11 Wagner, J. E., Jr. *et al.* Phase I/II Trial of StemRegenin-1 Expanded Umbilical Cord Blood Hematopoietic Stem Cells Supports Testing as a Stand-Alone Graft. *Cell Stem Cell* **18**, 144-155, doi:10.1016/j.stem.2015.10.004 (2016).

12 Bai, T. *et al.* Expansion of primitive human hematopoietic stem cells by culture in a zwitterionic hydrogel. *Nat Med* **25**, 1566-1575, doi:10.1038/s41591-019-0601-5 (2019).

13 Grey, W. *et al.* Activation of the receptor tyrosine kinase RET improves long-term hematopoietic stem cell outgrowth and potency. *Blood* **136**, 2535-2547, doi:10.1182/blood.2020006302 (2020).

14 Huang, J., Nguyen-McCarty, M., Hexner, E. O., Danet-Desnoyers, G. & Klein, P. S. Maintenance of hematopoietic stem cells through regulation of Wnt and mTOR pathways. *Nat Med* **18**, 1778-1785, doi:10.1038/nm.2984 (2012).

15 Wilkinson, A. C. *et al.* Long-term ex vivo haematopoietic-stem-cell expansion allows nonconditioned transplantation. *Nature* **571**, 117-121, doi:10.1038/s41586-019-1244-x (2019).

16 Wilkinson, A. C., Ishida, R., Nakauchi, H. & Yamazaki, S. Long-term ex vivo expansion of mouse hematopoietic stem cells. *Nat Protoc* **15**, 628-648, doi:10.1038/s41596-019-0263-2 (2020).

17 Ieyasu, A. *et al.* An All-Recombinant Protein-Based Culture System Specifically Identifies Hematopoietic Stem Cell Maintenance Factors. *Stem Cell Reports* **8**, 500-508, doi:10.1016/j.stemcr.2017.01.015 (2017).

18 Seita, J. *et al.* Lnk negatively regulates self-renewal of hematopoietic stem cells by modifying thrombopoietin-mediated signal transduction. *Proc Natl Acad Sci U S A* **104**, 2349-2354, doi:10.1073/pnas.0606238104 (2007).

19 Park, H. J. *et al.* Cytokine-induced megakaryocytic differentiation is regulated by genome-wide loss of a uSTAT transcriptional program. *EMBO J* **35**, 580-594, doi:10.15252/embj.201592383 (2016).

20 Yamazaki, S. *et al.* Cytokine signals modulated via lipid rafts mimic niche signals and induce hibernation in hematopoietic stem cells. *Embo j* **25**, 3515-3523, doi:10.1038/sj.emboj.7601236 (2006).

21 Miyamoto, K. *et al.* Foxo3a is essential for maintenance of the hematopoietic stem cell pool. *Cell Stem Cell* **1**, 101-112, doi:10.1016/j.stem.2007.02.001 (2007).

22 Tadokoro, Y. *et al.* Spred1 Safeguards Hematopoietic Homeostasis against Diet-Induced Systemic Stress. *Cell Stem Cell* **22**, 713-725.e718, doi:10.1016/j.stem.2018.04.002 (2018).

23 Lechman, E. R. *et al.* Attenuation of miR-126 activity expands HSC in vivo without exhaustion. *Cell Stem Cell* **11**, 799-811, doi:10.1016/j.stem.2012.09.001 (2012).

24 Sakurai, M., Takemoto, H., Mori, T., Okamoto, S. & Yamazaki, S. In vivo expansion of functional human hematopoietic stem progenitor cells by butyzamide. *Int J Hematol*, doi:10.1007/s12185-020-02849-2 (2020).

25 Nishimura, T. *et al.* Use of polyvinyl alcohol for chimeric antigen receptor T-cell expansion. *Exp Hematol* **80**, 16-20, doi:10.1016/j.exphem.2019.11.007 (2019).

26 Ito, M. *et al.* NOD/SCID/gamma(c)(null) mouse: an excellent recipient mouse model for engraftment of human cells. *Blood* **100**, 3175-3182, doi:10.1182/blood-2001-12-0207 (2002).

27 Linn, M. *et al.* Soluplus® as an effective absorption enhancer of poorly soluble drugs in vitro and in vivo. *Eur J Pharm Sci* **45**, 336-343, doi:10.1016/j.ejps.2011.11.025 (2012).

28 Jin, X., Zhou, B., Xue, L. & San, W. Soluplus(®) micelles as a potential drug delivery system for reversal of resistant tumor. *Biomed Pharmacother* **69**, 388-395, doi:10.1016/j.biopha.2014.12.028 (2015).

29 Sudo, K., Yamazaki, S., Wilkinson, A. C., Nakauchi, H. & Nakamura, Y. Polyvinyl alcohol hydrolysis rate and molecular weight influence human and murine HSC activity ex vivo. *Stem Cell Res* **56**, 102531, doi:10.1016/j.scr.2021.102531 (2021).

30 Ito, R. *et al.* Establishment of a human allergy model using human IL-3/GM-CSF-transgenic NOG mice. *J Immunol* **191**, 2890-2899, doi:10.4049/jimmunol.1203543 (2013).

31 Fares, I. *et al.* EPCR expression marks UM171-expanded CD34(+) cord blood stem cells. *Blood* **129**, 3344-3351, doi:10.1182/blood-2016-11-750729 (2017).

32 Lehnertz, B. *et al.* HLF expression defines the human hematopoietic stem cell state. *Blood* **138**, 2642-2654, doi:10.1182/blood.2021010745 (2021).

33 Aguilo, F. *et al.* Prdm16 is a physiologic regulator of hematopoietic stem cells. *Blood* **117**, 5057-5066, doi:10.1182/blood-2010-08-300145 (2011).

34 Che, J. L. C. *et al.* Identification and characterization of in vitro expanded hematopoietic stem cells. *EMBO Rep* **23**, e55502, doi:10.15252/embr.202255502 (2022).

35 García-Prat, L. *et al.* TFEB-mediated endolysosomal activity controls human hematopoietic stem cell fate. *Cell Stem Cell* **28**, 1838-1850.e1810, doi:10.1016/j.stem.2021.07.003 (2021).

36 Liang, R. *et al.* Restraining Lysosomal Activity Preserves Hematopoietic Stem Cell Quiescence and Potency. *Cell Stem Cell* **26**, 359-376.e357, doi:10.1016/j.stem.2020.01.013 (2020).

37 Lee-Six, H. *et al.* Population dynamics of normal human blood inferred from somatic mutations. *Nature* **561**, 473-478, doi:10.1038/s41586-018-0497-0 (2018).

38 Subramanian, A. *et al.* Gene set enrichment analysis: a knowledge-based approach for interpreting genome-wide expression profiles. *Proc Natl Acad Sci U S A* **102**, 15545-15550, doi:10.1073/pnas.0506580102 (2005).

Figure Legends:

Figure 1. Chemically-defined cytokine-free media maintains human hematopoietic stem/progenitor cells (HSPCs) ex vivo

(a) Ex vivo proliferation of 1000 mouse bone marrow (BM) c-Kit$^+$Sca-1$^+$Linage$^-$ (KSL) HSPCs or 1000 human cord blood-derived (CB) CD34$^+$CD38$^-$ HSPCs cultured with 10 ng/ml SCF and 100 ng/ml THPO in polyvinyl alcohol (PVA)-based media. Mean of five independent cultures. $^{**}P = 0.0034$; $^{***}P = 0.0001$; $^{****}P < 0.0001$.

(b) Single cell phosphorylation status of PI3K and AKT in mouse KSL and human CB CD34$^+$CD38$^-$ cultured with PVA-based media containing SCF and THPO. Mean of 30 cells. AFI: average fluorescence intensity. $^{****}P < 0.0001$.

(c) Fold change in total cell numbers of human-cord-blood-derived CD34$^+$CD38$^-$ cultured with SC79 or 740Y-P in addition to human 10 ng/ml SCF (S) and 100 ng/ml THPO (T) in PVA-based media conditions. The starting cell count was 1000. Mean of five independent cultures. $^{*}P = 0.0145$; $^{**}P = 0.0051$.

(d) Fold change in total and CD34$^+$ cell numbers after a 7-day culture of 2x10^4 human CB CD34$^+$ cells in PVA-based media containing 740Y-P and 100 ng/ml THPO (T) with or without 10 ng/ml SCF (S). Mean of three independent cultures.

(e) Fold change in total and CD34$^+$ cell numbers after a 7-day culture of 2x10^4 of human CB CD34$^+$ cells in PVA-based media containing 740Y-P and THPO (T) or butyzamide (Buty). Mean of three independent cultures. $^{**\dagger}P = 0.0020$; $^{**\ddagger}P = 0.0054$.

(f) Fold change in total and CD34$^+$ cell number after a 7-day culture of 2x10^4 human CB CD34$^+$ cells in PVA-based media containing 0-20 μM 740Y-P and 0.01-0.5 μM butyzamide. Mean of three independent cultures.

(g) Cell numbers and phenotypes during the culture of 2.5x10^3 human CB CD34$^+$ cells in PVA-based media containing 1 μM 740Y-P and 0.1 μM butyzamide. Mean $\pm$ S.D. of three independent cultures.

Statistical significance was calculated using an unpaired two-tailed *t*-test: n.s., not significant.

Figure 2. Long-term ex vivo expansion of human HSPCs in chemically-defined cytokine-free cultures

(a) Fold change in total and $CD34^+$ cell numbers after a 7-day culture of $2x10^4$ human CB $CD34^+$ cells in PVA-based media containing 750 nM SR-1 and/or 70 nM UM171 in addition to 2a media containing 1 µM 740Y-P and 0.1 µM butyzamide. Mean of three independent cultures. $^{**}P = 0.0095$.

(b) Total, $CD34^+$, and $CD41^+$ cell numbers after a 14-day culture of $2x10^4$ CB $CD34^+$ cells in PVA-based 2a media with or without 70 nM UM171. Mean of three independent cultures. $^{***}P = 0.004$; $^{****}P < 0.0001$.

(c) Fold change in total and $CD34^+$ cell numbers during a 30-day culture of $2x10^4$ CB $CD34^+$ cells in PVA-based media containing 1 µM 740Y-P, 0.1 µM butyzamide, and 70 nM UM171 (PVA-based 3a media). Mean of three independent cultures.

(d) Mean human $CD45^+$ PB chimerism in recipient NOG mice at 4-, 8- and 12-weeks following transplantation of $1x10^4$ fresh CB $CD34^+$ cells or the cells derived from a 10-day or 30-day culture of $1x10^4$ CB $CD34^+$ cells in PVA-based 3a media. n=5-6 mice per group. $^{*}P = 0.0401$; $^{***}P = 0.0001$; $^{****}P < 0.0001$.

(e) Mean 16-week human $CD45^+$ cell chimerism in the BM and spleen from mice described in (**d**). n=3 mice per group. $^{***}P = 0.0003$; $^{****}P < 0.0001$.

(f) Mean 16-week human $CD34^+$ cell chimerism in the BM and spleen from mice described in (**d**). n=3 mice per group. $^{*\dagger}P = 0.0116$; $^{*\ddagger}P = 0.0416$; .$^{**}P = 0.0055$.

Statistical significance was calculated using an unpaired two-tailed *t*-test or ANOVA. n.s., not significant.

Figure 3. Caprolactam polymer-based 3a media supports efficient human HSC expansion ex vivo

(a) Total cell numbers generated after 7-days culture of $2x10^4$ human CB $CD34^+$ cells in 3a media containing various synthetic polymers (see in ***Methods*** for details). No polymer (none) was used as a negative control. Mean ± S.D. of three independent cultures. n.d., not detected.

(b) Fold change in total and $CD34^+$ cell numbers during a 30-day culture of $2x10^4$ CB $CD34^+$ in 3a media containing PVA and/or polyvinyl caprolactam-polyvinyl acetate-polyethylene glycol graft copolymer (PCL-PVAc-PEG). Mean of three independent cultures. $*P = 0.0170$; $**^{\dagger}P = 0.0190$; $**^{\ddagger}P = 0.0012$; $**^{\S}P = 0.0013$; $**^{\|}P = 0.0023$; $***P = 0.0006$.

(c) Mean human $CD45^+$ PB chimerism in recipient NOG mice following transplantation of $1x10^4$ day-30 cells derived from CB $CD34^+$ cell cultured in 3a media containing PVA or PCL-PVAc-PEG (cultures initiated with $1x10^4$ cells). n=5 per group. Results from replicate experiments shown in **Supplementary Table 1**. Independent experiments performed with 2-3 human CB samples per experiment. $*P = 0.0424$.

(d, e) Mean 16-week human $CD45^+$ and $CD34^+$ cell chimerism in the BM and spleen from mice described in (**c**). n=5 per group.

(f, g) Mean human $CD45^+$ PB, BM and spleen chimerism in secondary recipient NOG mice following transplantation of $1x10^6$ cells derived from primary recipients, as describe in (**d, e**). n=5 per group. Results from replicate experiments shown in **Supplementary Table 2**.

(h) Human PB chimerism and phenotypes in humanized IL-3/GM-CSF-transgenic NOG mice at 16-weeks following transplantation of $1x10^4$ day-20 cells derived from CB $CD34^+$ cell cultured in 3a media containing PCL-PVAc-PEG (cultures initiated with $1x10^4$ cells). n=5 per group. $****P < 0.0001$.

(i) Frequency for each human $CD45^+$ cell subpopulation in the PB from mice described in (**h**). Mean ± S.D. of five mice per group.

Statistical significance was calculated using an unpaired two-tailed *t*-test: n.s., not significant.

Figure 4. Long-term selective expansion of functional human HSCs in 3a media

(a) Log_2-fold expression change of indicated HSC-associated genes. Mean ± S.D. of three independent cultures. $EPCR^+$ and $EPCR^-$ indicates $CD34^{high}EPCR^+$ cells and $CD34^{high}EPCR^-$ cells, respectively. $^{**\dagger}P = 0.0049$; $^{**\ddagger}P = 0.0043$; $^{**\S}P = 0.0022$; $^{***}P = 0.0006$.

(b, c) Results from gene set enrichment analysis (GSEA) for genes differentially expressed between $CD34^{high}EPCR^+$ and $CD34^{high}EPCR^-$ samples using gene sets for HSC genes (**b**) and mitochondrial oxidative phosphorylation-related genes (**c**). Statistical significance was calculated using an empirical phenotype-based permutation test procedure[38].

(d) UMAP plot of single-cell RNA sequencing data from 10-day expanded $CD34^+$ CB cells with 12 cell clusters annotated (see in ***Methods*** for details). Integrated cell map from cells cultured in PCL-PVAc-PEG based 3a media, StemSpan with SR-1 media, or StemSpan with UM171 media. Statistical significance was calculated using an empirical phenotype-based permutation test procedure[38].

(e) Cell distribution within PCL-PVAc-PEG based 3a cultures, StemSpan with SR-1 cultures, and StemSpan with UM171 cultures. Black dotted frames indicate the HSPC-HLF cell cluster. See **Extended Data Figure 6g** for a quantification of *HLF* expression.

(f) Schematic of the single HSC expansion assay.

(g) Mean number of cells derived from single human $CD34^+CD38^-CD90^+CD45RA^-CD49f^+$ CB cell after 7-days culture (n=96). Results from replicate experiments shown in **Supplementary Table 3**. Independent experiments performed with 2-3 human CB samples per experiment.

(h, i) Mean human $CD45^+$ PB and BM chimerism in recipient NOD.Cg-$Prkdc^{scid}$ $Il2rg^{tm1Sug}$ $Kit^{em1(V831M)Jic}$/Jic (W41/W41) mice following transplantation (n=10), as described in (**g**). Results from replicate experiments shown in **Supplementary Table 4**. Statistical significance was calculated using an unpaired two-tailed *t*-test.

Methods:

Mice. C57BL/6 mice were purchased from Sankyo Lab Service (Tsukuba, Japan) or bred in-house. Immunodeficient NOD/Shi-scid, IL-2Rγ^{null} (NOG), NOD.Cg-Prkdc^{scid} Il2rg^{tm1Sug} Kit$^{em1(V831M)Jic}$/Jic (W41/W41), and human IL-3/GM-CSF-transgenic NOG (NOG IL-3/GM-Tg) mice[30] were purchased from the Central Institute for Experimental Animals (Kanagawa, Japan).

NOG and W41/W41 mice were developed at the Central Institute for Experimental Animals. Kit-mutated NOG-W41 mice were established by genome editing using transcription activator-like effector nucleases (TALENs). Designed TALEN mRNA pairs (Forward; 5'-gtgttccgttctaggcac-3', and Reverse; 5'-atgctctctggtgccatc-3') and 100-bp single-strand oligonucleotide (ssOligo) containing a G to A point mutation in the kinase domain of the c-Kit locus[39] were purchased from Thermo Fisher Scientific (Waltham, MA, USA). TALEN mRNA (4 ng/μl) and ssOligo (15 ng/μl) were mixed and injected into NOG mouse embryo to generate NOG-W41 mice. All mice were housed in specific-pathogen-free conditions with free access to food and water. All animal experiments were performed in accordance with institutional guidelines and were approved by the Animal Care and Use Committee of the Institute of Medical Science, The University of Tokyo, the Laboratory Animal Resource Center, University of Tsukuba and the Institutional Animal Care and Use Committee of Central Institute for Experimental Animals.

Isolation of mouse cells. Bone marrow (BM) c-Kit^{+}Sca-1^{+}Lineage^{-} (KSL) cells were isolated from 8- to 12-week-old mice. Whole BM cells were stained with APC-conjugated anti-c-Kit antibody (eBioscience, San Diego, CA, USA) and c-Kit^{+} cells enriched using anti-APC magnetic beads and LS columns (Miltenyi Biotec). The c-Kit-enriched cells were then stained with PE-conjugated anti-Sca-1 (eBioscience), and a lineage antibody cocktail (biotinylated CD4, 1:200, CD8, 1:200, CD45R, 1:200, TER119, 1:100, LY-6G/LY-6C 1:200, and CD127; 1:100, all from eBioscience), followed by staining with FITC-CD34 and streptavidin-APC-eFluor 780 (eBioscience, 1:200). Cell populations were purified and sorted by FACS AriaII (BD Biosciences,

554 Franklin Lakes, NJ, USA) with BD FACS Diva software using propidium iodide as a
555 dead cell stain. Antibodies are described in **Supplementary Table 5.**
556
557 ***Human umbilical cord blood cells.*** Human umbilical cord blood-derived (CB) $CD34^+$
558 cells were purchased from StemExpress (Folsom, CA, USA). $CD34^+CD38^-$ cells were
559 purified by staining thawed $CD34^+$ cells with PE-Cy7-labeled anti-human CD34 (BD
560 Biosciences, 1:100) and V450-labeled anti-human CD38 (BD Biosciences, 1:100), then
561 sorted as described above. For detailed phenotypic HSC analysis, cells were stained with
562 PerCP-Cy5.5-labeled anti-human CD34 (BioLegend, San Diego, CA, USA, 1:100),
563 BV421-labeled anti-human CD38 (BD Biosciences, 1:100), PE-Cy7-labeled anti-human
564 CD90 (BD Biosciences, 1:100), APC-H7-labeled anti-human CD45RA (BD Biosciences,
565 1:100) and PE-labeled anti-human CD49f (BD Biosciences, 1:100), then sorted as
566 described above. Antibodies are described in **Supplementary Table 5.** For all
567 experiments, different lots of CBs were used. For the comparison of fresh and expanded
568 cells, a common lot of cord blood was used.
569
570 ***PVA and cytokine-based cell cultures.*** Human CB $CD34^+$ cells cultures were performed
571 using IMDM (Life Technologies, Carlsbad, CA, USA), 1% insulin-transferrin-selenium-
572 ethanolamine (ITSX; Life Technologies), 1% penicillin/streptomycin/glutamine (P/S/G;
573 Life Technologies), 0.1% Good Manufacturing Practice Grade polyvinyl alcohol (PVA;
574 Japan VAM&POVAL CO., LTD, Osaka, Japan), 10 ng/ml recombinant human SCF
575 (PeproTech, Rocky Hill, NJ, USA) and 100 ng/ml recombinant human THPO
576 (PeproTech), at 37°C with 5% CO_2. Cultures were supplemented with 740Y-P (CAS No.
577 236188-16-1; synthesized) and SC79 (CAS No. 305834-79-1; Sigma-Aldrich, St. Louis,
578 MO, USA), as indicated. Mouse cell cultures were performed using F12 media (Life
579 Technologies), 1% ITSX, 1% P/S/G, 10 mM HEPES (Life Technologies), 0.1% PVA, 10
580 ng/ml recombinant mouse SCF (PeproTech) and 100 ng/ml recombinant mouse THPO
581 (PeproTech), at 37 °C with 5% CO_2. U-bottomed 96-well tissue culture plates were used
582 in mouse and human comparative experiments. All other cultures were performed using
583 24-well flat-bottomed CellBIND® tissue culture plates (Corning, Corning, NY, USA;
584 Product Number 3337).

Signaling analysis. Phosphorylation status of signaling molecules was analyzed by fluorescent immunocytostaining. At indicated timepoints, cells were attached to poly-l-lysine-coated slides (Matsunami Glass, Osaka, Japan), then fixed with 4% paraformaldehyde and permeabilized with 0.1% Triton X-100. The cells were stained with phosphorylation-specific anti-PI3K, anti-Stat5, anti-AKT, anti-JAK2, anti-Stat3, anti-p38MAPK, and anti-p44/42MAPK antibodies (all from Thermo Fisher Scientific, Waltham, MA, USA). After washing with PBS, cells were stained with Alexa Fluor 488-conjugated goat anti-rabbit IgG antibody (CAS No. A11008, Invitrogen) and DAPI. Immunofluorescence images were obtained and analyzed using a Cellomics ArrayScan VTI HCS Reader (Thermo Scientific) as described previously[18,40]. All experiments were performed using mixture of five cord blood samples.

PVA-based cytokine-free cultures. Human CB $CD34^+$ cell cultures were performed using IMDM, 1% ITSX, 1% P/S/G, 0.1% PVA, 740Y-P and butyzamide (Shionogi, Osaka, Japan) at 37 °C with 5% CO_2. All long-term cultures used 1 μM 740Y-P and 0.1 μM butyzamide, with media changes made every 3 days by manually removing conditioned media by pipetting and replacing pre-warmed and freshly prepared media. Butyzamide is a THPO receptor agonist[41,42] and has also been used clinically as a lusutrombopag. All cell cultures were performed using 24-well flat-bottomed CellBIND® tissue culture plates. Where indicated, cultures were supplemented with 750 nM StemRegenin 1 (SR-1; CAS No. 1227633-49-9) and/or 70 nM UM171 (CAS No. 1448724-09-1). As described in the main text, we defined media containing 1 μM 740Y-P, 0.1 μM butyzamide and 70 nM UM171 as 3a media.

PCL-PVAc-PEG-based cytokine-free cultures. A step-by-step protocol describing the culture of human CB $CD34^+$ cells with PCL-PVAc-PEG-based cytokine-free media can be found at Protocol Exchange[43]. Human CB $CD34^+$ cell cultures were performed using IMDM, 1% ITSX, 1% P/S/G, 1 μM 740Y-P, 0.1 μM butyzamide and 0.1% of polyvinyl caprolactam-polyvinyl acetate-polyethylene glycol graft copolymer (PCL-PVAc-PEG; Soluplus®; BASF, Ludwigshafen am Rhein, Germany) at 37 °C with 5% CO_2. For long-

term cultures, media changes made every 3 days by manually removing conditioned media by pipetting and replacing pre-warmed and freshly prepared media. For polymer screening, human CB $CD34^+$ cells were cultured with IMDM, 1% ITSX, 1% P/S/G, 1 µM 740Y-P, 0.1 µM butyzamide and 0.1% one of the following chemicals: PVA, 188 BIO (Kolliphor® P 188 Bio; BASF), 188 Geismar (Kolliphor® P188; BASF), PCL-PVAc-PEG, 407 Geismar (Kolliphor® P407; BASF), 30 Geismar (Kollidon® 30, BASF), 17 PF (Kollidon® 17 PF; BASF), 90 F (Kollidon® 90 F; BASF) or 12 PF (Kollidon® 12 PF; BASF) at 37 °C with 5% CO_2. In addition, PCL-PVAc-PEG-based cytokine cocktails media consisted of 10 ng/ml recombinant mouse SCF (PeproTech) and 100 ng/ml recombinant mouse THPO (PeproTech) (described in **Extended Data Figure 4a**).

UM171 and/or SR-1-based cultures. Human CB $CD34^+$ cell cultures for xenotransplantation assays were performed using StemSpan SFEM (Stem Cell Technologies, Vancouver, BC, Canada) supplemented with 100 ng/ml recombinant human SCF (PeproTech), 100 ng/ml FMS-like tyrosine kinase 3 ligand (FLT3, PeproTech), 50 ng/ml recombinant human THPO (PeproTech), 10 µg/ml lipoproteins (Stem Cell Technologies) and 35nM UM171 and/or 750nM SR-1 at 37 °C with 5% CO_2 (**Extended Data Figure 4f-i**) [10]. In comparison experiments with previously protocols, human CB $CD34^+$ cell cultures were performed using StemSpan SFEM supplemented with 50 ng/ml recombinant human SCF (PeproTech), 50 ng/ml FLT3-L, 50 ng/ml recombinant human THPO, 50 ng/ml recombinant human IL-6 (PeproTech) and 750nM SR-1 at 37 °C with 5% CO_2 (described in **Figure 4e**, **Extended Data Figure 4a-e, Extended Data Figure 5a, Extended Data Figure 6g**) [11].

Analysis of cell cultures. Cultured cells were counted using a hemocytometer or a CYTORECON cytometer (GE Healthcare, Amersham, UK) before and after culture. Phenotypic analysis was performed by staining cells with PE-Cy7-labeled anti-human CD34 (1:100), V450-labeled anti-human CD38 and FITC-labeled anti-human CD41 (BioLegend, 1:100), followed by flow cytometric analysis using a FACS AriaII or FACS Verse (BD Biosciences) with BD FACS Diva software using propidium iodide as a dead stain. For detailed phenotypic HSC analysis, fresh or cultured cells were stained with

PerCP-Cy5.5-labeled anti-human CD34 (BioLegend, 1:100), BV421-labeled anti-human CD38 (BD Biosciences, 1:100), PE-Cy7-labeled anti-human CD90 (BD Biosciences, 1:100), APC-H7-labeled anti-human CD45RA (BD Biosciences, 1:100), PE-labeled anti-human CD49f (BD Biosciences, 1:100), FITC-labeled anti-human lineage cocktail (CD2, CD3, CD4, CD7, CD8, CD10, CD11b, CD14, CD19, CD20, CD56, CD235a) (BD Biosciences, 1:200) and FITC-labeled (BioLegend, 1:200) or BV711-labeled (BD Biosciences, 1:100) anti-human CD41**,** followed by flow cytometric analysis using a FACS AriaIII (BD Biosciences) with BD FACS Diva software using propidium iodide as a dead stain. As a set of markers containing EPCR, cultured cells were stained with APC-labeled anti-human CD34 (BioLegend, 1:100), BV421-labeled anti-human CD90 (BioLegend, 1:100), PerCP-Cy5.5-labeled anti-human CD45RA (BioLegend, 1:20), PE-labeled anti-human CD49c (ITGA3) (BD Biosciences, 1:200), BV605-labeled anti-human CD201 (EPCR) (BD Biosciences, 1:100) and FITC-labeled anti-human lineage cocktail. Antibodies are described in **Supplementary Table 5.** Results were analyzed with FlowJo software 10.8.1 (Tree Star, Ashland, OR).

Colony forming unit (CFU) assays. Defined numbers of fresh or cultured cells were sorted by FACS AriaII and subjected to CFU assays using Methocult H4435 (Stem Cell Technologies). Cells were incubated in a humidified atmosphere at 37 °C with 5% CO_2. After two weeks, the number of colonies were counted and types of colonies were validated by cytospin smears stained with Hemacolor (Merck, Darmstadt, Germany).

Xenotransplantation assays. Fresh or cultured human CB $CD34^+$ cells were transplanted by tail artery injection[44] into sub-lethally (1.5 Gy) irradiated 8-10-week-old immunodeficient NOD/Shi-scid IL-2Rγ^{null} (NOG) mice or NOG IL-3/GM-Tg mice. Human cell chimerism in the peripheral blood analyzed using V450–labeled anti-mouse CD45.1 (BD Biosciences, 1:200) and APC-Cy7–labeled anti-human CD45 antibodies (BioLegend, 1:100) following red blood cell lysis. Mice were randomly selected and BM and spleen analysis was performed. Human $CD34^+$ cell chimerism in the BM and spleen was determined using V450–labeled anti-mouse CD45.1 (1:200), APC-Cy7–labeled anti-human CD45 antibodies (1:100), and PE–labeled anti-human CD34 (BioLegend, 1:50).

For detailed phenotypic HSC analysis, cells were stained with PerCP-Cy5.5-labeled anti-human CD34 (BioLegend, 1:100), BV421-labeled anti-human CD38 (BD Biosciences, 1:100), PE-Cy7-labeled anti-human CD90 (BD Biosciences, 1:100), APC-H7-labeled anti-human CD45RA (BD Biosciences, 1:100) and PE-labeled anti-human CD49f (BD Biosciences, 1:100)**.** Human lineage chimerism in the BM and spleen was determined using V450–labeled anti-mouse CD45.1, APC-Cy7–labeled anti-human CD45 antibodies, PE-Cy7-labeled anti-human CD33 (eBioscience, 1:20), PE-labeled anti-human CD3 (eBioscience, 1:20), and APC–labeled anti-human CD19 (eBioscience, 1:100). We defined $CD33^+$ cells as myeloid cells, $CD19^+$ cells as B cells, and $CD3^+$ cells as T cells. In xenotransplantation assays using NOG IL-3/GM-Tg mice (described in **Figure 3h, i**), we used PE-labeled anti-human CD56 (BioLegend, 1:100) and FITC-labeled anti-human CD66b (BioLegend, 1:100) additionally. Flow cytometry analysis was then performed using a FACS AriaII or FACS Verse (BD Biosciences) with propidium iodide as dead stain, and results were analyzed with FlowJo software. For secondary transplantation assays, we collected and pooled bone marrow from all primary recipient mice at 16 weeks and transplanted $1x10^6$ cells into each sub-lethally-irradiated NOG mice as described above, with donor chimerism analyzed as above. In xenotransplantation assays using W41/W41 and NOG mice (described in **Extended Data Figure 8**), $5x10^4$ fresh human CB $CD34^+$ cells were transplanted into W41/W41, W41/+ or +/+ mice with or without irradiation, with donor chimerism analyzed as above.

Clonal HSC expansion assays. Single human CB-derived $CD34^+CD38^-CD90^+CD45RA^-CD49f^+$ cells were purified by staining thawed PerCP-Cy5.5-labeled anti-human CD34 (BioLegend, 1:100), BV421-labeled anti-human CD38 (BD Biosciences, 1:100), PE-Cy7-labeled anti-human CD90 (BD Biosciences, 1:100), APC-H7-labeled anti-human CD45RA (BD Biosciences, 1:100) and PE-labeled anti-human CD49f (BD Biosciences, 1:100) then sorted single cell into a 96-well flat-bottomed CellBIND® tissue culture plate. After culturing with PCL-PVAc-PEG-based 3a media for 7 days as described above, the top 10 wells with high expansion efficiency were transplanted into sub-lethally (1 Gy) irradiated 8-10-week-old W41/W41 mice by tail artery injection (detailed in **Figure 4f**). For split clone transplantation assays, after culturing with PCL-PVAc-PEG-based 3a

media for 7 days as described above, each of the 6 wells with highest expansion efficiency were transplanted into three sub-lethally (1 Gy) irradiated 8-10-week-old W41/W41 mice by tail artery injection (detailed in **Extended Data Figure 7a, b**).

Thrombopoietin receptor agonist screening. MPL-expressing 32D cells culture were performed using RPMI media containing 1% ITSX, 1% P/S/G, and 0.1% BSA or PVA at 37 °C with 5% CO_2. One of the following thrombopoietin receptor agonists was added to each culture: 7 μM eltrombopag (Cayman Chemical Company, Ann Arbor, MI, USA); 3 μM avatrombopag (MedChemExpress, Monmouth Junction, NJ, USA); or 0.1 μM butyzamide[41]. Human CB $CD34^+$ cell cultures were performed using IMDM, 1% ITSX, 1% P/S/G, 0.1% PVA, 740Y-P, and one of the following thrombopoietin receptor agonist: 7 μM eltrombopag, 3 μM avatrombopag, or 0.1 μM butyzamide at 37 °C with 5% CO_2.

Preparation and culture of human peripheral blood stem cells. Fresh human peripheral blood stem cells (PBSCs) were obtained from healthy adult donors for allogeneic transplantation in the University of Tsukuba Hospital (approval R02-009). The donors received the treatment of G-CSF before leukapheresis. All donors agreed to experimental use of their PBSCs after informed consent and our study was approved by the ethical committee in the University of Tsukuba. From PBSCs, mononuclear cells (MCs) were separated by Lymphocytes Separation Medium 1077 (PromoCell, CAS No. C-44010). After separation, $CD34^+$ cells were enriched using the Human CD34 Microbeads Kit (Miltenyi Biotec Inc., CAS No. 130-046-702) and MACS LS columns (Miltenyi Biotec Inc., CAS No. 130-042-401). Purified $CD34^+$ cells were cultured in PVA- and PCL-PVAc-PEG based 2a or 3a media. In 3a media cultures, UM729 (1 μM) was used in place of UM171 because UM171 was not commercially available at the time this experiment was performed. All experiments complied with all relevant guidelines and regulations.

Exome Sequencing. We extracted genomic DNA of fresh and 10-day cultured human CB $CD34^+$ cells using QIAamp DNA Blood Mini Kit (QIAGEN, CAS No. 51106). After DNA fragmentation, target enrichment by hybrid capture probes was performed using SureSelect Human All Exon V6 (Agilent). Enriched DNA was sequenced on NovaSeq

6000 (Macrogen Inc, Korea). FASTQ files were imported to CLC Genomics Workbench (ver. 10.1.1) for subsequent analysis. Sequence data was annotated using the reference genome (GRCh38). After filtering out common variants using the database of Tohoku Medical Megabank Organization (https://www.megabank.tohoku.ac.jp), we annotated mutations unique to the culture sample that were located in amino-acid change sites or splicing sites.

Bulk RNA sequencing. Human CB $CD34^+$ cells were cultured in PCL-PVAc-PEG based 3a media at 37°C with 5% CO_2 for 10-days. $CD34^{high}EPCR^+$ and $CD34^{high}EPCR^-$ cells were then sorted by MoFlo XDP (Beckman Coulter) and processed in TRIZOL-LS (Thermo Fisher Scientific, 10296028). Total RNA was used for rRNA-depletion by NEBNExt rRNA Depletion Kit (New England Biolabs, CAS No. E6310), and next directional library synthesis by NEBNext Ultra Directional RNA Library Prep Kit for Illumina (New England Biolabs, CAS No. E7420). Libraries were sequenced on Illumina NextSeq 5000. We analyzed the data using the edgeR v3.14[45] in R (4.1.1). Volcano plots were generated using EnhancedVolcano (https://github.com/kevinblighe/EnhancedVolcano) in R and genes highlighted when the value of $\log_2$ fold change was >2 and $-\log_{10}P$ was >14. Gene Ontology enrichment analysis was performed by ClusterProfiler[46]. Gene set enrichment analysis (GSEA) software (http://www.gsea-msigdb.org/gsea/index.jsp) was used for comparing our datasets with two previously published datasets.

Single-cell RNA sequencing. Human CB $CD34^+$ cells were cultured for 10-days at 37°C with 5% CO_2 under three different conditions as follows: (1) PCL-PVAc-PEG based 3a media (composition described above); (2) StemSpan SFEM (Stem Cell Technologies, Vancouver, BC, Canada) supplemented with 100 ng/ml recombinant human SCF (PeproTech), 100 ng/ml FMS-like tyrosine kinase 3 ligand (FLT3, PeproTech), 50 ng/ml recombinant human THPO (PeproTech), 10 µg/ml lipoproteins (Stem Cell Technologies) and 35 nM UM171[2]; and (3) StemSpan SFEM supplemented with 50 ng/ml recombinant human SCF (PeproTech), 50 ng/ml FLT3-L, 50 ng/ml recombinant human THPO, 50 ng/ml recombinant human IL-6 (PeproTech) and 750 nM SR-1[11]. From each CB cell

771 culture, the propidium iodide-negative fraction was sorted by MoFlo (Beckman Coulter)
772 and single cell Gel Beads-in-Emulsions were generated using the Chromium Controller
773 (10x Genomics). Libraries were generated using the Single Cell 3' Reagent Kit version
774 3.1 (10x Genomics) according to manufacturer's instructions.
775 Cells were sequenced on Illumina Hiseq X (Macrogen Inc, Korea). Sequence data
776 was annotated by the reference genome (GRCh38) using the Cellranger v6.1.1 pipeline.
777 Subsequent analysis was performed using Seurat v4.047 in R. Using the Read10X
778 function, we obtained the unique molecular identified (UMI) count matrix of each dataset.
779 This analysis identified 9913 cells for the PCL-PVAc-PEG sample, 5912 cells for the
780 UM171 sample, and 9198 cells for the SR-1 sample. The mean reads per cell was 32205
781 for the PCL-PVAc-PEG sample, 36026 for the UM171 sample, and 30991 for the SR-1.
782 The median number of genes detected per cell was 3292 genes for the PCL-PVAc-PEG
783 sample, 3648 genes for the UM171 sample, and 3300 genes for the SR-1 sample. We
784 filtered out cells that had unique feature counts of over 7500 or less than 200, and cells
785 with >10% mitochondrial counts. The filtered cell count number (cells used for
786 subsequent analysis) was 9572 cells for the PCL-PVAc-PEG sample, 5373 cells for the
787 UM171 sample, and 6991 cells for the SR-1 sample, with 22179 features, 21222 features,
788 and 21645 features detected, respectively.
789 Normalization and scaling were performed with the SCTransform function
790 (method = “glmGamPoi”). At this time, the effect of the mitochondrial gene expression
791 ratio was removed (var.to.regress = “percent.mt”). The SelectIntegrationFeatures
792 (nfeatures = 3000) function was used to select genes for integration of the datasets. After
793 processing the datasets with the PrepSCTIntegration function, FindIntegrationAnchors
794 and IntegrateData functions were used to find anchors for integration and integrate the
795 datasets. To correct for cell-to-cell variation due to the effects of cell cycle, cell cycle
796 scoring and regression was performed with CellCycleScoring function, using a published
797 mouse hematopoietic stem cells dataset[47]. Scaling was then performed with the ScaleData
798 (vars.to.regress = c("S.Score", "G2M.Score")) function. Principal components analysis
799 (PCA) was performed using the RunPCA function (npc = 30). Uniform Manifold
800 Approximation and Projection (UMAP) was performed using the RunUMAP function to
801 reduce the dimension of the dataset of embedded cells into two dimensions.

FindNeighbors function was used to determine k-nearest neighbors (KNN) for each cell, and the KNN graph was constructed based on Euclidean distance. Finally, processed cells were clustered based on KNN using the Louvain algorithm (resolution = 0.4) by the FindCluster function. FindMarkers and FindAllMarkers functions were used to identify intercluster differentially expressed genes and select feature genes that characterized specific hematopoietic cell types. This allowed for the follow clusters to be manually annotation: hematopoietic stem/progenitor cells highly expressing *HLF* (HSPC-HLF), hematopoietic stem/progenitor cells (HSPC), cell-cycle activated hematopoietic stem/progenitor cells (HSPC-Cycling), granulocyte-monocyte progenitor cells (GMP), monocyte progenitor cells (MP), granulocyte progenitor cells (GP), dendritic cell progenitors (DCP), CD34 and *GATA2*-expressing progenitor cells ($CD34^+GATA2^+$ prog), megakaryocyte and erythroid progenitor cells (MEP), erythroid progenitor cells (EryP), megakaryocyte progenitor cells (MgkP), and mast cell progenitors (MCP).

Subsequent analysis was performed using Seurat v4.0[48] in R. Fresh CB data for the comparison of *HLF* expression in cultured cells (**Extended Data Figure 6g**) was obtained from GEO (GSE 153370)[32]. In addition, we compared our datasets with GEO-deposited scRNAseq data from 7-day cultured CB $CB34^+$ cells in StemSpan SFEM + UM171 (GSE 153370). We filtered out cells (with feature counts over 7500 or less than 200, and those with >10% mitochondrial counts) and used NormalizedData, CellCycleScoring and ScaleData functions to process data. Next, FindTransferAnchors was performed to find anchors between our datasets (as reference data) and the published datasets (as query data). After the RunUMAP function (reduction.model = TRUE) was applied to the reference data, MapQuery function was used to perform Unimodal UMAP Projection (**Extended Data Figure 6f**).

Cell Cycle analysis. Cultured human CB $CD34^+$ cells were stained with APC-labeled anti-human CD34 (BioLegend), PerCP-Cy5.5-labeled anti-human CD45RA (BioLegend), then washed with phosphate-buffered saline (PBS) twice and pelleted. BD Cytofix/Cytoperm Fixation/Permeabilization Kit (BD Biosciences, 554714) was then used to process the samples according to manufacturer's instructions. After fixation and permeabilization, the cells were stained with FITC-labeled anti-human Ki67 (BioLegend,

1:100) and DAPI (DOJINDO, 1:1000). FITC-labeled IgG2b kappa (BioLegend, 1:100) was used as an isotype control. Antibodies are described in **Supplementary Table 5.** Analysis was performed on a LSR Fortessa Cell Analyzer (BD Bioscience). Data was analyzed with FlowJo software.

Apoptosis assay. Suspension of cultured human CB $CD34^+$ cells were centrifuged and washed by PBS. Next, annexin binding buffer (10mM HEPES, 140mM NaCl and 2.5mM $CaCl_2$ diluted in distilled water) was added to the sample. After that, the cells were stained by AlexaFluor488 AnnexinV (Invitrogen, 1:40) and propidium iodide (BioLegend1:1000) and incubated for 15 minutes at room temperature. Antibodies are described in **Supplementary Table 5.** Finally, we resuspended the samples in the annexin binding buffer and analyzed them by LSR Fortessa Cell Analyzer (BD Biosciences).

Reactive Oxygen Species (ROS) Assay. Fresh and cultured cells were pre-stained with APC-labeled anti-human CD34 (BioLegend, 343510). The cells were then processed with a ROS Assay Kit-Photo-oxidation Resistant DCFH-DA (DOJINDO, R253) according to the manufacturer's instructions. Cell samples were incubated in the Working Buffer for 30 minutes at 37°C with 5% CO_2 and then washed with HBSS twice. Analysis was performed on a Attune NxT Flow Cytometer (Invitrogen). Data was analyzed with FlowJo software.

γH2A.X Assay. Fresh and cultured cells were pre-stained with APC-labeled anti-human CD34 (BioLegend, 343510). The cells were then processed with BD Cytofix/Cytoperm Fixation/Permeabilization Kit (BD Biosciences, 554714) according to the manufacturer's instructions and intracellularly stained with FITC-labeled anti-H2A.X Phospho (Ser139) antibody (BioLegend, 613404, 1:100). Analysis was performed on a Attune NxT Flow Cytometer (Invitrogen). Data was analyzed with FlowJo software.

Statistical analysis. Statistical analysis was performed using two-tailed t-testing or ANOVA in Prism 9 software (GraphPad, San Diego, CA, USA).

Data Availability Statement: Exome sequencing data available on BioProject (PRJNA786760). All RNA-seq data were deposited in the Gene Expression Omnibus under accessions GSE191338 (bulk) and GSE192519 (single cell). Source data are provided with this paper.

Additional references:

39 Nocka, K. *et al.* Molecular bases of dominant negative and loss of function mutations at the murine c-kit/white spotting locus: W37, Wv, W41 and W. *Embo j* **9**, 1805-1813 (1990).

40 Ema, H. *et al.* Adult mouse hematopoietic stem cells: purification and single-cell assays. *Nat Protoc* **1**, 2979-2987, doi:10.1038/nprot.2006.447 (2006).

41 Nogami, W. *et al.* The effect of a novel, small non-peptidyl molecule butyzamide on human thrombopoietin receptor and megakaryopoiesis. *Haematologica* **93**, 1495-1504, doi:10.3324/haematol.12752 (2008).

42 Sakurai, M., Takemoto, H., Mori, T., Okamoto, S. & Yamazaki, S. In vivo expansion of functional human hematopoietic stem progenitor cells by butyzamide. *Int J Hematol* **111**, 739-741, doi:10.1007/s12185-020-02849-2 (2020).

43 Sakurai, M., Ishitsuka, K. & Yamazaki, S. Cytokine-free ex vivo expansion of human hematopoietic stem cells. *Protoc. Exch.*

44 Kuchimaru, T. *et al.* A reliable murine model of bone metastasis by injecting cancer cells through caudal arteries. *Nat Commun* **9**, 2981, doi:10.1038/s41467-018-05366-3 (2018).

45 Robinson, M. D., McCarthy, D. J. & Smyth, G. K. edgeR: a Bioconductor package for differential expression analysis of digital gene expression data. *Bioinformatics* **26**, 139-140, doi:10.1093/bioinformatics/btp616 (2010).

46 Wu, T. *et al.* clusterProfiler 4.0: A universal enrichment tool for interpreting omics data. *Innovation (N Y)* **2**, 100141, doi:10.1016/j.xinn.2021.100141 (2021).

47 Nestorowa, S. *et al.* A single-cell resolution map of mouse hematopoietic stem and progenitor cell differentiation. *Blood* **128**, e20-31, doi:10.1182/blood-2016-05-716480 (2016).

48 Hao, Y. *et al.* Integrated analysis of multimodal single-cell data. *Cell* **184**, 3573-3587.e3529, doi:10.1016/j.cell.2021.04.048 (2021).

Acknowledgements: We thank M. Watanabe, Y. Yamazaki, Y. Ishii, M. Hayashi, R Hirochika, M. Kikuchi and Organization for Open Facility Initiatives, University of Tsukuba for excellent technical support, and Y. Niitsu, M. Kawakatsu, T.Kajiura, K.

Kolter and F. Guth for providing polymers. This research was funded by JSPS KAKENHI Grant-in-Aid for Scientific Research (JP20H03707; JP20H05025; JP20K17407) and the Japan Agency for Medical Research and Development (AMED) (21bm0404077h0001; 21bm0704055h0002). M.S. is supported by JSPS KAKENHI Grant-in-Aid for Scientific Research (JP20K17407), the Japanese Society of Hematology Research Grant (19056, 20128) and Nippon Shinyaku Research Grant. A.C.W. is supported by the Kay Kendall Leukaemia Fund, the NIHR, the Leukemia and Lymphoma Society (3385-19), and NIH (K99HL150218). H.J.B. is supported by the German Research Foundation (BE 6847/1-1). H.N. is supported by the California Institute for Regenerative Medicine (grantsLA1_C12-06917), the US National Institutes of Health (grants R01DK116944, R01HL147124 and R21AG061487), JSPS KAKENHI Grant-in-Aid for Scientific Research, and the Virginia and D.K. Ludwig Fund for Cancer Research.

Author contributions: M.S., K.I. and S.Y. conceived, designed and performed experiments, analyzed data and wrote the paper. R.I., T.K., E.M., H.N., K.S., H.J.B. and H.T. designed and performed experiments. M.S. performed cell cultures, colony-forming unit assays and FACS analysis, and xenotransplantation assays. K.I. performed cell cultures, FACS analysis, exome sequencing, RNA sequencing, cell cycle analysis, apoptosis assays, ROS assays, and γH2A.X assays, S.Y performed cell cultures, signaling analysis, xenotransplantation assays, and clonal HSC expansion assays, R.I. performed xenotransplantation assays, T.K. performed exome sequencing and RNA sequencing, E.M., H.N, K.S. H.J.B. and H.T. helped with cell cultures and FACS analysis. S.Y. performed independent replications of the experiments (Supplementary Table 1-4) both in the University of Tokyo, University of Tsukuba, and R.I. performed independent replications of the experiment (Supplementary Table 1-2) in Central Institute for Experimental Animals. A.C.W. and D.G.K. analyzed data and wrote the paper. T.S. provided reagents and discussed the results. K.K., S.T., Y.N., A.I., S.C. and S.O. discussed the results and wrote the paper. H.N. guided and supervised the project. All authors edited and approved the paper.

Competing interests: M.S and S.Y are co-founders and shareholders in Celaid Therapeutics. H.N. is a co-founder and shareholder in Megakaryon, Century Therapeutics and Celaid Therapeutics. All other authors declare no competing interests.

Supplementary Information: This file contains Supplementary Tables 1-5.

Materials and Correspondence: Satoshi Yamazaki, y-sato4@md.tsukuba.ac.jp; Hiromitsu Nakauchi, nakauchi@stanford.edu

Extended data figures and tables: 8 Extended Data Figures and 2 Extended Data Tables available in the online version of the paper.

Extended Data Figure Legends:

Extended Data Figure 1: Development of chemically-defined cytokine-free culture media for human hematopoietic stem/progenitor cells (HSPCs)

(a) Single cell phosphorylation status of JAK2, STAT3, STAT5, p38 MAPK, and p44/42 MAPK in mouse KSL and human CB $CD34^+CD38^-$ cells cultured with 10 ng/ml SCF and 100 ng/ml THPO in PVA-based media. Mean of 30 cells. AFI: average fluorescence intensity. ****$P < 0.0001$.

(b) Representative image of p-PI3K after 7-days culture cells in mouse and human, as described in **(a)**. Blue: DAPI, Green：anti-PI3K. Scale bar: 100 μm.

(c) Single cell phosphorylation status of PI3K in mouse $CD34^-$KSL and human $CD34^+CD38^-CD90^+CD45RA^-CD49f^+$ CB cells cultured with 10 ng/ml SCF and 100 ng/ml THPO in PVA-based media for 3 and 7 days. Mean of 31 cells. AFI: average fluorescence intensity. ****$P < 0.0001$.

(d) $CD34^+CD45RA^-$ cell numbers of human-cord-blood-derived $CD34^+CD38^-$ cultured with SC79 or 740Y-P in addition to human 10 ng/ml SCF (S) and 100 ng/ml THPO (T) in PVA culture conditions for 7 days. The starting cell count was $2x10^4$. Mean of three independent cultures. **$P = 0.0040$.

(e) Single cell phosphorylation status of PI3K in human $CD34^+CD38^-CD90^+CD45RA^-CD49f^+$ CB cells cultured in PVA-based media containing 10 ng/ml SCF and 100 ng/ml THPO with or without 740Y-P for 7 days. Mean of 31 cells. AFI: average fluorescence intensity. ***$P = 0.0002$.

(f) Cell cycle analysis of $CD34^+CD45RA^-$ cells after a 7-day culture of human CB $CD34^+$ cells in PVA-based media containing 740Y-P and 100 ng/ml THPO (T) with or without 10 ng/ml SCF (S). Mean of three independent cultures. Representative FACS plot was shown on the right.

(g) Fold change in GEmM colony numbers generated from human CB $CD34^+$ cells after a 7-day culture in PVA-based media supplemented with 740Y-P and THPO (T) with or without SCF (S), relative to fresh $CD34^+$ cells. Mean of three independent cultures.

(h) Total cell numbers after $1x10^3$ MPL-expressing 32D cells (32D/MPL) were cultured for 3-days with various THPO agonists (eltrombopag, avatrombopag or butyzamide) in BSA-based or PVA-based media. Mean of two independent cultures. n.d., not detected.

(i) Fold change in total and $CD34^+$ cell numbers after a 7-day culture of $2x10^4$ $CD34^+$ cells in PVA-based media supplemented with 740Y-P and various THPO agonists (eltrombopag, avatrombopag or butyzamide). Mean of three independent cultures. n.d., not detected.

(j) $CD34^+$ $CD41^-$ $CD90^+CD45RA^-$ cell numbers after a 7-day culture of $2x10^4$ of human CB $CD34^+$ cells in PVA-based media containing 740Y-P and 100 ng/ml THPO (T) and/or butyzamide (Buty). Mean of three independent cultures. $^{**}P = 0.0020$; $^{***}P = 0.0010$.

(k) Fold change in GEmM colony numbers generated from $CD34^+$ cells after a 7-day culture in PVA-based media supplemented with 740Y-P and THPO (T) or butyzamide (Buty), relative to fresh $CD34^+$ cells. Mean $\pm$ S.D. of three independent cultures. $^{**}P = 0.0017$.

(l) The frequency of cells during the culture of $2x10^4$ human CB $CD34^+$ cells in PVA-based media containing 1 μM 740Y-P and 0.1 μM butyzamide. Mean $\pm$ S.D. of three independent cultures.

(m) Representative image of a day-14 PVA-based culture containing 1 μM 740Y-P and 0.1 μM butyzamide (2a media). Representative of at least five experiments. Scale bar: 100 μm.

(n) Megakaryocytic (MgK) colony numbers obtained from 50 $CD34^+$ cells sorted from day 7 and day 14 PVA-based cultures containing 1 μM 740Y-P and 0.1 μM butyzamide (2a media). Mean $\pm$ S.D. of three independent cultures. $^{*}P = 0.0161$.

(o, p) Mean human $CD45^+$ peripheral blood (PB) and BM chimerism in recipient NOD/Shi-scid IL-2Rγ^{null} (NOG) mice following transplantation of $1x10^4$ cells derived from a 7-day or 14-day culture of $1x10^4$ CB $CD34^+$ cells in PVA-based 2a media containing 1 μM 740Y-P and 0.1 μM butyzamide. n=5 mice per group. **(o)** $^{**\dagger}P = 0.0036$; $^{**\ddagger}P = 0.0037$; $^{***}P = 0.0007$, **(p)** $^{***}P = 0.0003$.

Statistical significance was calculated using an unpaired two-tailed t-test. n.s., not significant.

Extended Data Figure 2: Long-term ex vivo expansion of human HSPCs in chemically-defined cytokine-free cultures

(a) $CD34^+$ $EPCR^+$ cell numbers after a 7-day culture of $2x10^4$ human CB $CD34^+$ cells in PVA-based media containing 750 nM SR-1 and/or 70 nM UM171 in addition to 2a media. Mean of three independent cultures. ****$P < 0.0001$.

(b) $CD34^+$ $EPCR^+$ and $CD34^+EPCR^+CD90^+CD45RA^-ITGA3^+$ cell numbers after a 14-day culture of $2x10^4$ CB $CD34^+$ cells in PVA-based 2a media with or without 70 nM UM171. Mean of three independent cultures. ****$P < 0.0001$.

(c) The frequency of $CD34^+EPCR^+CD90^+CD45RA^-ITGA3^+$ cells after a 10-day culture of $2x10^4$ human CB $CD34^+$ cells in StemSpan SFEM supplemented with cytokines with 35 nM UM171 and PVA-based 2a media with 35 or 70 nM UM171. Mean of three independent cultures. ****$P < 0.0001$.

(d) Annexin V staining assay of total cells after a 7-day culture of $2x10^4$ human CB $CD34^+$ cells in PVA-based media containing 750 nM SR-1 and/or 0.1% BSA in addition to 2a or 10 ng/ml SCF (S) and 100 ng/ml THPO (T). Mean of three independent cultures. ****$P < 0.0001$.

(e) Mean human $CD45^+$ PB chimerism in recipient NOG mice at 24 weeks following transplantation of $1x10^4$ fresh CB $CD34^+$ cells or the cells derived from a 10-day or 30-day culture of $1x10^4$ CB $CD34^+$ cells in PVA-based 3a media. n=3 mice per group. Details described in **Figure 2d**. *$^{\dagger}P = 0.0495$; *$^{\ddagger}P = 0.0319$.

(f) Mean 24-week human $CD45^+$, $CD34^+$, $CD34^+CD38^-CD90^+CD45RA^-CD49f^+$ cell chimerism in the BM from mice described in (**e**). n=3 mice per group. Details described in **Figure 2d.** *$^{\dagger}P = 0.0112$; *$^{\ddagger}P = 0.0480$; *$^{\S}P = 0.0187$; **$P = 0.0075$; ***$P = 0.0003$; ****$P < 0.0001$.

(g) Mean 24-week human $CD45^+$, $CD34^+$, $CD34^+CD38^-CD90^+CD45RA^-CD49f^+$ cell chimerism in the spleen from mice described in (**e**). n=3 mice per group. Details described in **Figure 2d.** **$P = 0.0014$.

Statistical significance was calculated using one-way ANOVA or an unpaired two-tailed *t*-test. n.s., not significant.

Extended Data Figure 3: Caprolactam polymer-based 3a media supports efficient expansion of human HSCs ex vivo

(a) $CD34^+CD45RA^-$ cell numbers of human-cord-blood-derived $CD34^+$ cultured with SC79 or 740Y-P in addition to human 10 ng/ml SCF (S) and 100 ng/ml THPO (T) in PCL-PVAc-PEG culture conditions for 7 days. The starting cell count was $2x10^4$. Mean of three independent cultures. *P = 0.0210.

(b) $CD34^+CD41^-CD90^+CD45RA^-$ cell numbers after a 7-day culture of $2x10^4$ human CB $CD34^+$ cells in PCL-PVAc-PEG-based media containing 740Y-P and 100 ng/ml THPO (T) and/or butyzamide (Buty). Mean of three independent cultures. *P = 0.0256.

(c) $CD34^+EPCR^+$ and $CD34^+EPCR^+CD90^+CD45RA^-$ cell numbers after a 7-day culture of $2x10^4$ human CB $CD34^+$ cells in PCL-PVAc-PEG -based 2a media containing 750 nM SR-1 and/or 70 nM UM171 . Mean of three independent cultures. **P = 0.0021; ***P = 0.0002.

(d) $CD34^+CD41^-CD90^+CD45RA^-$ cell numbers after a 7-day culture of $2x10^4$ of human CB $CD34^+$ cells in PCL-PVAc-PEG-based media containing 0-20 µM, 740Y-P, and 0.1 µM butyzamide. Mean of three independent cultures. *$^{\dagger}P$ = 0.0214; *$^{\ddagger}P$ = 0.0440.

(e) The frequency of $CD34^+EPCR^+CD90^+CD45RA^-ITGA3^+$ cells after a 7-day culture of $2x10^4$ human CB $CD34^+$ cells in PCL-PVAc-PEG-based 2a media with 35 nM or 70 nM UM171. Mean of three independent cultures.

(f) GEmM colony numbers generated from $CD34^+$ cells after a 10-day culture in PVA- and/or PCL-PVAc-PEG-based 3a media. Mean of three independent cultures. ***P = 0.0005.

(g) Annexin V staining assay of total cells after a 7-day culture of $2x10^4$ human CB $CD34^+$ cells in PVA- or PCL-PVAc-PEG-based 2a media containing 750 nM SR-1. Mean of three independent cultures. **P = 0.0086.

(h) The frequency of PI positive cells after a 7-day culture of $2x10^4$ human CB $CD34^+$ cells in PCL-PVAc-PEG-based 3a media with or without 10 µM LY294002 (Chemscene, CAS No. 154447-36-6), PI3-kinase inhibitor. Mean of three independent cultures. ****P < 0.0001.

(i) Total and $CD34^+EPCR^+CD90^+CD45RA^-ITGA3^+$ cell numbers after a 10-day culture of $2x10^4$ adult-peripheral blood stem cell (PBSC) $CD34^+$ cells in PVA- or PCL-PVAc-PEG-based 3a media including UM729 instead of UM171. Mean of three independent cultures. *P=0.0153, **P=0.0079.

(j) Mean human $CD45^+$ PB chimerism in recipient NOG mice at 24 weeks after transplantation of $1x10^4$ day-30 cells derived from CB $CD34^+$ cells cultured in 3a media containing PVA or PCL-PVAc-PEG. n=3 mice per group. Detailed described in **Figure 3c.**

(k) Mean 24-week human $CD45^+$, $CD34^+$, $CD34^+CD38^-CD90^+CD45RA^-CD49f^+$ cell chimerism in the BM from mice described in (**j**). n=3 mice per group. Detailed described in **Figure 3c.**

(l) Mean 24-week human $CD45^+$, $CD34^+$, $CD34^+CD38^-CD90^+CD45RA^-CD49f^+$ cell chimerism in the spleen from mice described in (**j**). n=3 mice per group. Detailed described in **Figure 3c.**

Statistical significance was calculated using one-way ANOVA or an unpaired two-tailed *t*-test: n.s., not significant.

Extended Data Figure 4: Comparison of human HSC culture protocols

(a) Total cell numbers generated from a 10-day culture of $2x10^4$ human CB $CD34^+$ cells in PCL-PVAc-PEG or StemSpan SFEM-based cytokine-cocktail media with UM171 and/or SR-1 (see in ***Methods*** for details), or PCL-PVAc-PEG-based 3a media. Mean of three independent cultures. $^{***}P = 0.0002$; $^{****}P < 0.0001$.

(b) The frequency and **(c)** absolute number of $CD34^+EPCR^+CD90^+CD45RA^-ITGA3^+$ cells in cultures described in (**a**). Mean of three independent cultures. **(b)** $^{****}P < 0.0001$. **(c)** $^{**}P = 0.0010$; $^{***\dagger}P = 0.0009$; $^{***\ddagger}P = 0.0002$; $^{****}P < 0.0001$.

(d) The ROS and γH2AX level of fresh CB $CD34^+$ cells (fresh) and $CD34^+$ cells in cultures described in (**a**). Mean of three independent cultures. $^{**}P = 0.0028$; $^{***}P = 0.0004$; $^{****}P < 0.0001$.

(e) Relative mean fluorescence intensity (MFI) for ROS and yH2AX in fresh CB $CD34^+$ cells (fresh) and cells from 10 or 30 day PCL-PVAc-PEG-based 3a media cultures. Mean of three independent cultures.

(f, g) Mean human $CD45^+$ PB and BM chimerism in recipient NOG mice following transplantation of $1x10^4$ day-10 cells derived cultures as describe in (**a**). n=4 mice per group. $^{***}P = 0.0001$; $^{****}P < 0.0001$.

(h, i) Mean human $CD45^+$ PB and BM chimerism in secondary recipient NOG mice following transplantation of $1x10^6$ BM cells derived from primary recipient mice, as describe in (**f, g**). n=3 mice per group. $*^{\dagger}P = 0.0180$; $*^{\ddagger}P = 0.0299$.
Statistical significance was calculated using one-way ANOVA: n.s., not significant.

Extended Data Figure 5: Gating strategy for HSCs fraction by flow cytometry

(a) FACS gating strategy for detecting $CD34^+EPCR^+CD90^+CD45RA^-ITGA3^+$ cells after 10-day culture in 3a media containing PCL-PVAc-PEG or using UM171/SR-1.

Extended Data Figure 6: Profile of human HSCs expanded in 3a media

(a) Volcano plot showing differentially expressed genes (DEGs) detected in bulk RNA-sequencing of $CD34^{high}EPCR^+$ (right) and $CD34^{high}EPCR^-$ (left) cells after 10-day culture in PCL-PVAc-PEG based 3a media. DEGs are highlighted as red dots ($log_2FC > 2$, $-logP$ Value <14). Gene names are shown in the boxes.
(b) GO Term cellular component-specific GSEA analysis performed on DEGs, displayed as a dotplot.
(c) Expression of key genes within annotated clusters, displayed as a dotplot.
(d, e) Feature plots showing *HLF* (c) and *AVP* (d) gene expression within the integrated cell map.
(f) Ratio of each cell cluster within PCL-PVAc-PEG based 3a cultures, StemSpan with SR-1 cultures, and StemSpan with UM171 cultures, as described in **Figure 4e**.
(g) Comparison of scRNAseq data from cells cultured for 10 days in PCL-PVAc-PEG based 3a media with two dataset of cells cultured for 7 days in StemSpan SFEM with UM171 cultures obtained from GEO (GSE 153370).
(h) Violin plots displaying *HLF* expression in cells from a 10-day culture using 3a media, cells from UM171/SR-1 cultures, and two fresh CBs from publicly available data (GSE 153370).

Extended Data Figure 7: Split clone assays

(a) Schematic of assay of the single HSC expansion and split clone assay. Single human $CD34^+CD38^-CD90^+CD45RA^-CD49f^+$ CB cells were sorted into 96 wells and expanded

in 3a media containing PCL-PVAc-PEG for 7 days. Individual HSC clones were then transplanted into three recipient W41/W41 mice.

(b) Human $CD45^+$ PB chimerism in recipient W41/W41 mice 24 weeks after transplantation of day-7 cells derived from single human $CD34^+CD38^-CD90^+CD45RA^-CD49f^+$ CB cell cultured in 3a media containing PCL-PVAc-PEG (3 mice/well), as described in (**a**).

Extended Data Figure 8: NOG-W41/W41 mice display high human hematopoietic cell chimerism

(a) Mean human $CD45^+$ PB chimerism in recipient NOD.Cg-Prkdc^{scid} Il2rg^{tm1Sug} Kit$^{em1(V831M)Jic}$/Jic (W41/W41), W41/+, +/+ mice at 4, 8, 12, 16 and 20 weeks following transplantation of $5x10^4$ fresh CB $CD34^+$ cells. n=3-4 mice per group. ***P = 0.0004; ****P <0.0001.

(b) Mean 24-week human $CD45^+$ cell chimerism in the BM and spleen from mice described in (**a**). n=3-4 mice per group. **$^{\dagger}P$ = 0.0016; **$^{\ddagger}P$ = 0.0021; ***$^{\dagger}P$ = 0.0001; ***$^{\ddagger}P$ = 0.0006.

(c) Mean human $CD45^+$, $CD19^+$, $CD33^+$, $CD3^+$, $CD56^+$ and $CD66b^+$ PB chimerism in recipient non-irradiated or irradiated (0.5 Gy) W41/W41 mice at 4-, 8-, 12- and 16-weeks following transplantation of $5x10^4$ fresh CB $CD34^+$ cells. Mean ± S.D of 3-4 mice per group. *$^{\dagger}P$ = 0.0257; *$^{\ddagger}P$ = 0.0335; **$^{\dagger}P$ = 0.0030; **$^{\ddagger}P$ = 0.0060; ***P = 0.0002.

Statistical significance was calculated using one-way ANOVA or an unpaired two-tailed *t*-test: n.s., not significant.

Extended Data Table 1: Detailed data of xenotransplantation assays

(a) Mean ± S.D 16-week frequency of $CD33^+$ myeloid cells, $CD3^+$ T cells, and $CD19^+$ B cells of human $CD45^+$ cells in the BM and spleen of mice described in **Figure 2e**.

(b) Mean ± S.D 16-week frequency of $CD33^+$ myeloid cells, $CD3^+$ T cells, and $CD19^+$ B cells of human $CD45^+$ cells in the BM and spleen of mice described in **Figure 3d.**

(c) Mean ± S.D 24-week frequency of $CD33^+$ myeloid cells, $CD3^+$ T cells, and $CD19^+$ B cells of human $CD45^+$ cells in the PB of mice described in **Figure 4i**.

Extended Data Table 2: Whole exome sequencing on uncultured and 10-day cultured cells. Whole exome sequencing on fresh CB and 10-day cultured CB CD34+ cells with PCL-PVAc-PEG-based 3a medium.

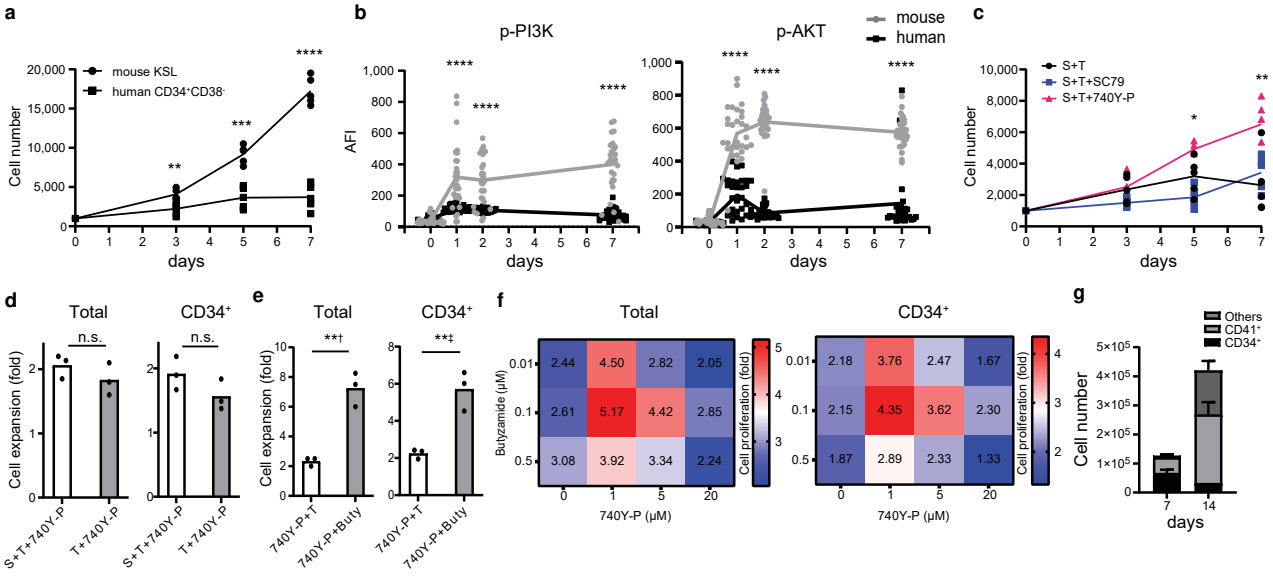

Figure 1 Sakurai, et al.

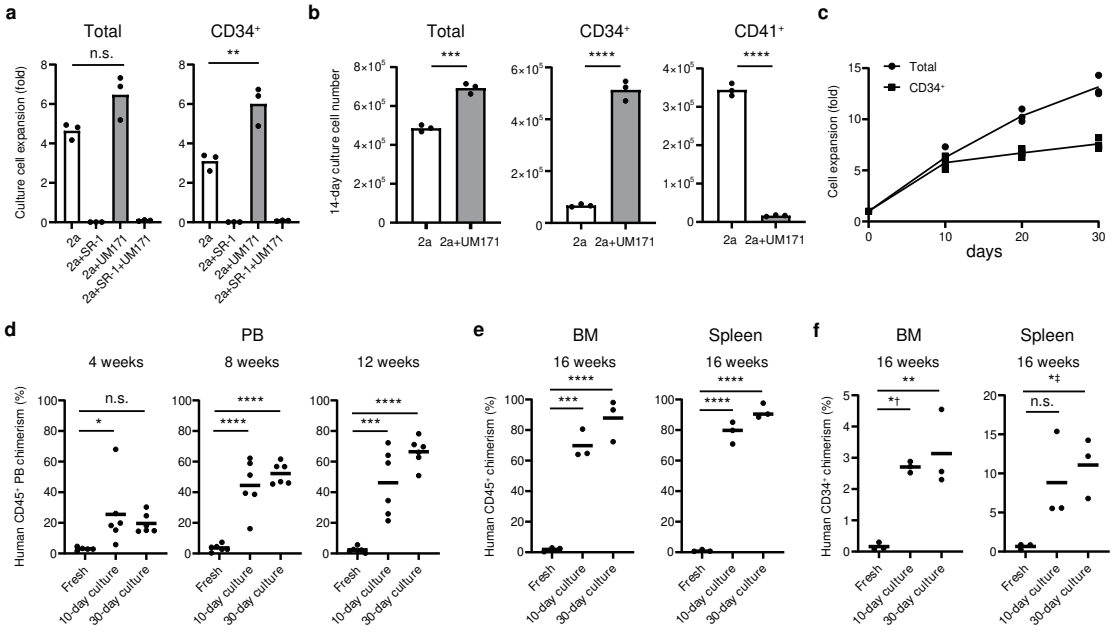

Figure 2 Sakurai, et al.

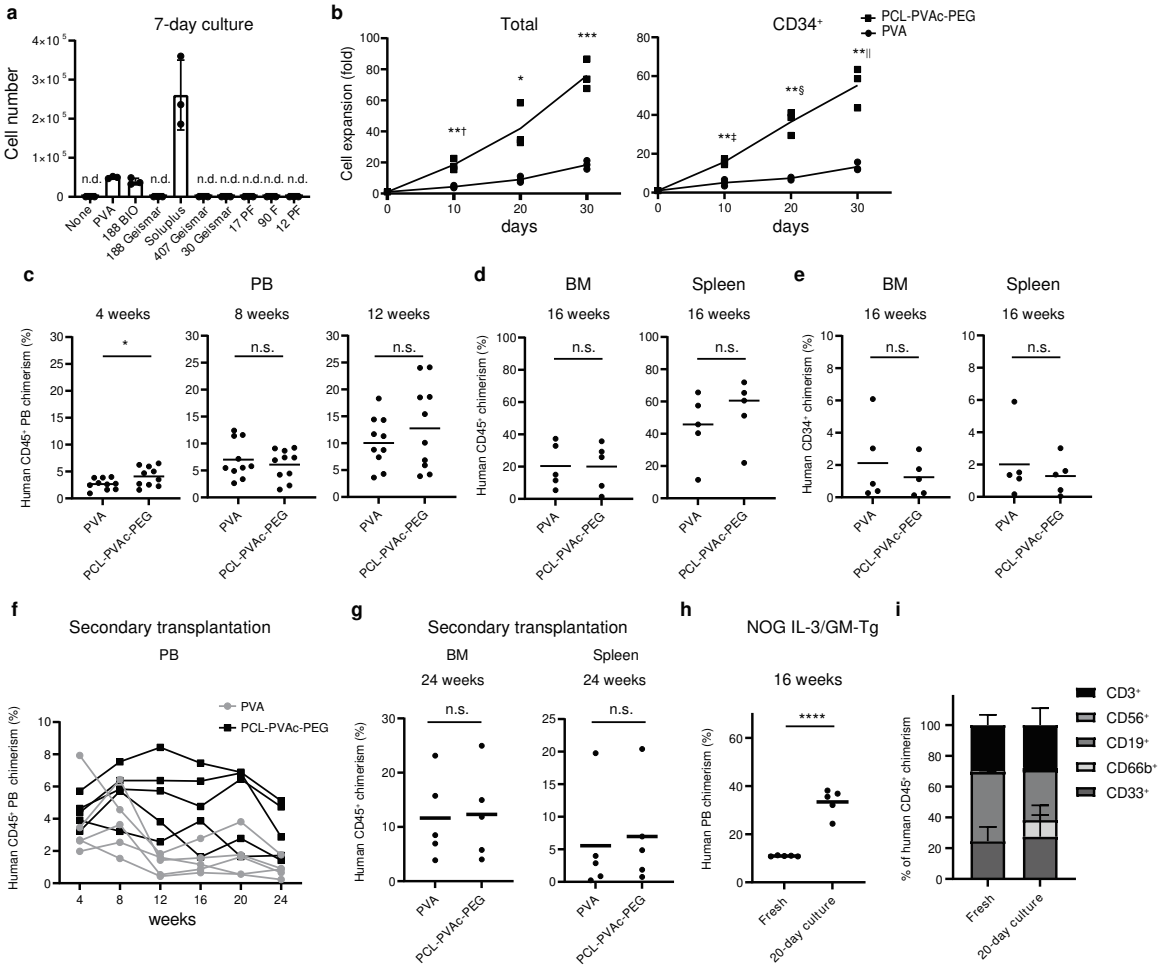

Figure 3 Sakurai, et al.

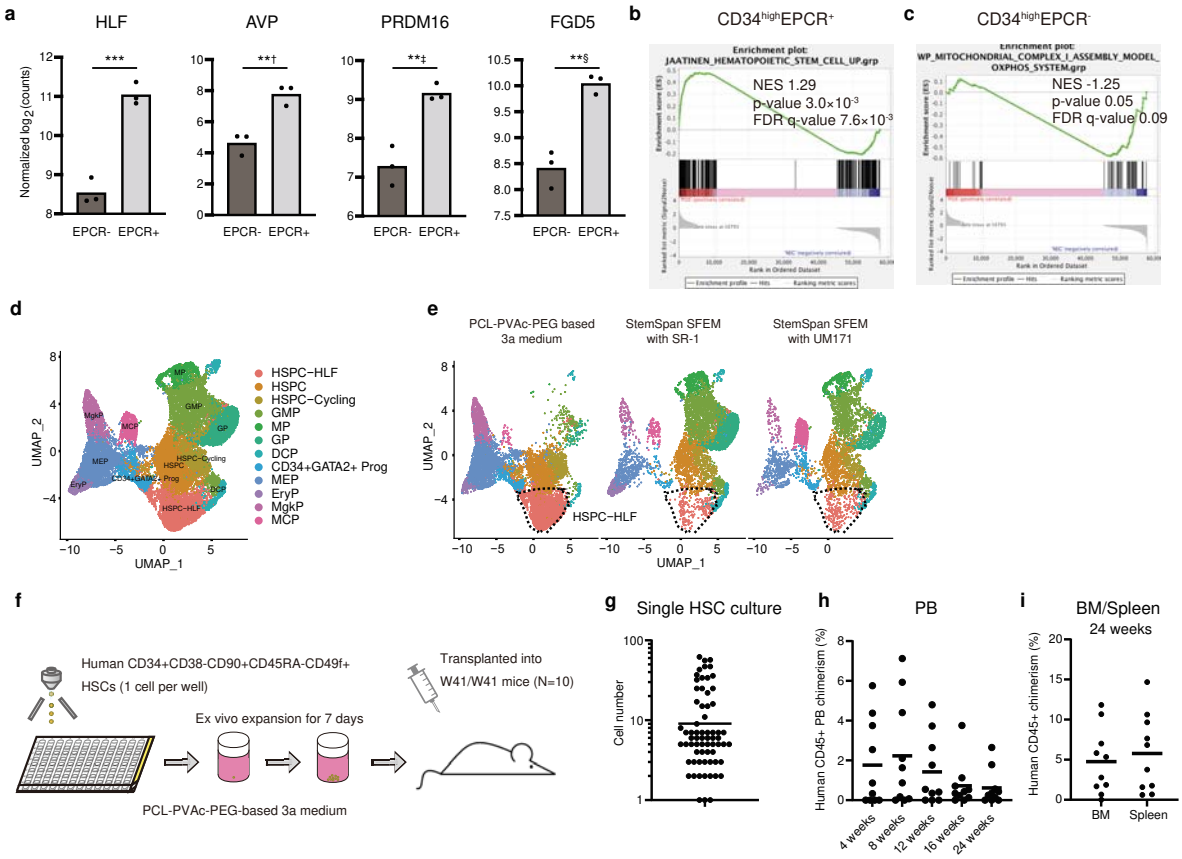

Figure 4 Sakurai, et al.